

Constrained motions and slow dynamics in one-dimensional bosons with double-well dispersion

Yang-Zhi Chou* and Jay D. Sau

Condensed Matter Theory Center and Joint Quantum Institute,
Department of Physics, University of Maryland, College Park, Maryland 20742, USA
(Dated: June 2, 2023)

We investigate the dynamical properties of one-dimensional interacting bosons with double-well dispersion, which can be realized in the ultracold atom experiments. We demonstrate slow dynamics and constrained motion of domain walls in the low-temperature symmetry-broken regime. The constrained domain-wall motion is “fracton-like” – a single domain wall cannot move freely, while two nearby domain walls can move collectively. Such an unusual property stems from the emergent dipole moment conservation in the symmetry-broken regime. Consequently, we find an Ohmic-like linear response and a vanishing superfluid stiffness, which are atypical for gases in a disorder-free background in one dimension - but similar to a 2D superfluid with free vortices. In addition, we develop a hydrodynamic description for the dynamics controlled by the interacting quantum Lifshitz critical point and obtain superfluid stiffness $\rho_s \sim T$ and sound velocity $v_s \sim T^{1/2}$, showing qualitatively similar low-temperature dynamics to the symmetry-broken regime. Our results reveal several unprecedented dynamical properties relevant to the fractons and explain the stable domain walls in the existing experiments.

I. INTRODUCTION

Ultracold neutral atom systems have been a promising platform for studying novel quantum many-body phenomena. Particularly, the ability to control interacting bosons motivates substantial new fundamental research [1–14] that don’t have solid-state analogs. For example, interacting bosons with double-well dispersion (with two dispersion minima at $k = \pm k^*$) can be realized in the experiments [6, 10, 12] with at least three distinct approaches — One can achieve double-well dispersion by using two counter-propagating Raman laser lights which effectively create spin-orbit coupling for the pseudospin-1/2 bosons [6, 15, 16]. Alternatively, a bosonic ladder with π flux per plaquette (by laser-assisted tunneling [17]) generates double-well dispersion with the chain degrees of freedom acting like the pseudospins [18–20]. Lastly, shaking an optical lattice with a frequency close to the energy difference between the ground band and the first excited band can realize double-well dispersion [10, 12]. Interacting bosons with double-well dispersion allow for rich quantum phase diagrams and novel dynamical response [21–37].

Bose condensates with double-well dispersion are highly nontrivial, even without internal degrees of freedom (e.g., pseudospin). Owing to the nature of two dispersion minima, a Z_2 symmetry-breaking phase transition (analogous to an Ising ferromagnetic transition [6]) occurs at low temperatures for repulsively interacting bosons. Topological defects appear as domain walls separating regimes with different momentum. Intriguingly, the domain walls are stable and can persist for hundreds of milliseconds in the experiments [10, 12], imply-

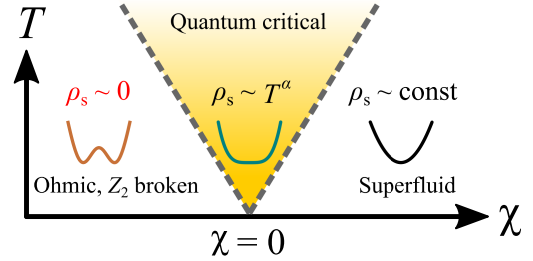


FIG. 1. Phase diagram and superfluid stiffness (ρ_s). $\chi \propto -B$ is the control parameter of the quantum phase transition. For $\chi > 0$, a dispersion with single minima is realized. ρ_s is finite and essentially temperature-independent. For $\chi < 0$, the dispersion develops two minima at $\pm k^*$, and a spontaneous Z_2 breaking takes place. ρ_s vanishes in this regime, and the corresponding transport is Ohmic-like. At $\chi = 0$, a Lifshitz dispersion (i.e., a k^4 dispersion) manifests. The superfluid stiffness $\rho_s \sim T^\alpha$ with $\alpha = 1$.

ing slow relaxation in the low-temperature (but $T \neq 0$) symmetry-broken regime.

In this work, we study the dynamics of one-dimensional (1D) interacting single-component bosons with double-well dispersion as summarized in Fig. 1. Under spontaneous Z_2 symmetry breaking, the system naturally realizes multiple domains carrying finite momenta, k^* or $-k^*$. We demonstrate that the motion of domain walls are highly constrained. A single domain wall cannot move, while two nearby domain walls can move in a collective fashion. Such intriguing kinetic properties are due to the *emergent* dipole moment conservation, which suggests a genuine connection to the “fractons” [38–57]. We also develop a linear response theory for the state with multiple domain walls and show vanishing superfluid stiffness and Ohmic transport, despite being a Bose condensate. Such results should be contrasted with the

* yzchou@umd.edu

hydrodynamics controlled by an interacting fixed point, where superfluid stiffness and sound velocity vanish at zero temperature. Our theory provides a natural explanation for the stable domain walls in experiments [10, 12] and suggests a potential (albeit not rigorous) connection to fracton phenomenology.

II. MODEL

The 1D interacting single-component bosons with a double-well dispersion are described by

$$\hat{H} = \int dx \left[-B|\partial_x b|^2 + C|\partial_x^2 b|^2 - \mu|b|^2 + \frac{U}{2}|b|^4 \right] \quad (1)$$

where b is the annihilation operator for a boson, B and $C > 0$ are the coefficients controlling single-particle dispersion, μ is the chemical potential, and $U > 0$ denotes the repulsive short-range interaction. In this Letter, we focus mainly on the $B > 0$ scenario, which admits a double-well dispersion with two minima at $k = \pm k^* = \pm\sqrt{B/(2C)}$ and an energy barrier $\epsilon_0 = B^2/(4C)$ at $k = 0$. $B = 0$ is a critical point that realizes a Lifshitz dispersion (i.e., k^4). For $B < 0$, the problem is qualitatively similar to the well-known repulsive Lieb-Liniger model [3, 4, 58, 59] (upto some dispersion correction).

The 1D bosons with a double-well dispersion realize a rich phase diagram with two tunable dimensionless parameters, $\gamma = U/(B\rho_0)$ (with ρ_0 being the density) and $\delta = \mu/\epsilon_0$. γ is the dimensionless interaction parameter analogous to the dimensionless parameter in the Lieb-Liniger model [3, 4, 58, 59]. Different from the Lieb-Liniger model, a quantum phase transition separates $\gamma \ll 1$ and $\gamma \gg 1$ regimes because of the Z_2 character of the double-well dispersion [30].

In this Letter, we focus only on the superfluid phase (i.e., $\gamma \ll 1$). Since there are two dispersion minima ($k = \pm k^*$), it is important to determine the ground state configuration. With mean-field approximation, one can show that the ground state is the same as the ‘‘plane-wave phase’’ in the 1D spin-orbit-coupled BEC [16], where only one minimum is occupied. As a result, the ground state features a spontaneous Z_2 symmetry breaking, and the ground state degeneracy is two. We adopt the standard harmonic fluid approximation in the high-density superfluid limit [60] such that the complex boson field is decomposed into the density and phase fields as follows:

$$b(x) \approx \sqrt{n_0 + \delta n(x)} e^{i\phi(x)}, \quad (2)$$

where n_0 is the averaged density, δn encodes the local fluctuation of density, and ϕ is the phase field. Using the expression of b in Eq. 2, we can rewrite Eq. (1) with the two dynamical variables, ϕ and δn . For $|\delta n| \ll n_0$, we can integrate out δn_0 in the imaginary-time path integral and obtain a phase-only action. After rescaling of the parameters, we obtain an imaginary-time action \mathcal{S}_{eff} (See

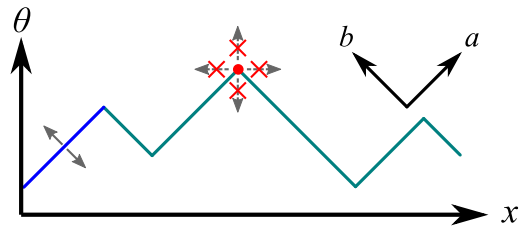


FIG. 2. Motion of domain wall in the symmetry-broken phase. In each domain, $|\partial_x \theta| = m_0$, where $m_0 = \sqrt{|r|/(4u)}$. A single domain wall (e.g., the red dot) cannot move freely because of the energy penalty, while an entire domain (e.g., the blue segment) can move. The directions of collective coordinate a and b are also marked in the figure. The domain-wall positions are labeled by x_n .

Appendix A for derivations and extended discussions) given by

$$\mathcal{S}_{\text{eff}} \approx \int d\tau dx \left[\frac{1}{2}(\partial_\tau \theta)^2 + \frac{1}{2}(\partial_x^2 \theta)^2 + \frac{r}{2}(\partial_x \theta)^2 + u(\partial_x \theta)^4 \right], \quad (3)$$

where τ is the rescaled imaginary time, θ is the rescaled phase field, $r \propto -B$, and u is the effective interaction of the phase fields. Equation (3) is strictly valid for $\delta \gg 1$. For $\delta \ll 1$, density fluctuation cannot be ignored near a domain wall [29]. One can show that u becomes negative for $\delta < 8$, indicating that higher order terms such as $(\partial_x \theta)^6$ are needed for the phase-only action. We restrict our analysis for $\delta \gg 1$, i.e., $u > 0$. (We will comment on the other limit in the discussion.)

III. Z_2 SYMMETRY-BROKEN REGIME

The 1D bosons with a double-well dispersion manifest spontaneous Z_2 symmetry breaking, analogous to a ferromagnetic transition. To see this, we first define $m(x) = \partial_x \theta$. The static part of Eq. (3) becomes the standard Landau theory for an Ising magnet, $\frac{r}{2}m^2 + \frac{1}{2}(\partial_x m)^2 + um^4$. For $r < 0$, the $\langle m \rangle \neq 0$ features a spontaneous symmetry breaking. At zero temperature, the m is spatially uniform, and $|m| = m_0 = \sqrt{|r|/(4u)}$. At small finite temperatures, the system develops multiple domains with alternating signs of m (corresponding to the slope of θ) as illustrated in Fig. 2. The density of domain walls is proportional to $\exp(-E_{\text{DW}}/T)$, where E_{DW} is the energy cost for creating one domain wall [29]. The relaxation in a state with multiple domain walls is highly unusual as discussed in the following.

A. Domain walls and constrained motion

First, we discuss the single-domain-wall solution. In the θ -representation, an up-pointing single-domain-wall

solution is described by [29]

$$\theta_{\text{DW}}(x) = \theta_0 + m_0 \sqrt{\frac{2}{|r|}} \ln \left[\cosh \left(\sqrt{\frac{|r|}{2}} (x - x_0) \right) \right], \quad (4)$$

where the domain wall position is at x_0 . When $\sqrt{|r|}|x - x_0| \gg 1$, the domain wall solution recovers the slope m_0 for $x > x_0$ and $-m_0$ for $x < x_0$. Remarkably, moving a single domain wall will violate the energy constraint in Hamiltonian by forcing slopes to deviate from the equilibrium value $\pm m_0$. Thus, the motion of a single domain wall is suppressed due to the potential energy. However, one can move the entire domain while satisfying the potential energy (the blue segment in Fig. 2). As a result, two nearby domain walls can move simultaneously. The constrained domain-wall motion here is a direct consequence of momentum conservation (i.e., spatial translation invariant) of the 1D interacting bosons with double-well dispersion. Since the domain is between two phases with different center of mass momenta, shifting the domain-wall requires a perturbation with a finite force.

To understand the constrained domain-wall motion further, we examine the states with multiple domains more closely in the following. First, we label the two type of domain walls to positive charge (up-pointing) and negative charge (down-pointing). The total dipole moment is given by

$$\mathcal{D} = \sum_n (x_{2n} - x_{2n-1}), \quad (5)$$

where x_n indicates the position of the n th domain wall (as illustrated in Fig. 2). Then, we assume $\frac{\theta(x_{n+1}) - \theta(x_n)}{x_{n+1} - x_n} = (-1)^{n+1} m_0$ without loss of generality. Using this configuration, we can show that

$$\mathcal{D} = m_0 \sum_n [\theta(x_{2n}) - \theta(x_{2n-1})] = 2\pi Q m_0, \quad (6)$$

where Q is a constant dictating the boundary condition. Thus, the total dipole moment \mathcal{D} is a conserved quantity associated with the boundary condition of θ . The conservation of dipole moment suggests a relation to the fractons [38–57] which is known for its constrained dynamics of excitations. We discuss the consequence due to the constrained domain-wall dynamics next.

B. Casimir force and phonon drag

An essential consequence of the constrained domain-wall motion is the unusually slow relaxation. Since domain-wall diffusion is forbidden, the primary relaxation mechanism is due to phonon excitations and collective domain motion (i.e., the simultaneous motion of two nearby domain walls), which we discuss in the following.

We are interested in the interplay between a long-wavelength variation of θ (i.e., a long-wavelength “phonon” mode) and a domain wall. A particularly interesting question is how phonons are scattered by domain walls and how domain walls are affected by phonons. To answer this question, we consider a long-wavelength variation $\delta\theta(x)$ on top of a single domain-wall profile θ_{DW} [Eq. (4)]. We can construct a solution such that the entire $x < x_0$ domain displaces slightly (corresponding to the blue domain motion in Fig. 2) while the $x > x_0$ domain remains the same. For $|x| \sqrt{|r|/2} \gg 1$ (i.e., sufficiently away from the domain wall), we find that $\delta\theta(x \rightarrow -\infty) \neq 0$ and $\delta\theta(x \rightarrow \infty) = 0$, corresponding to a perfect reflection at the domain wall. (See Appendix B for a discussion.) The phonons in each domain couple through the motion of the domain walls. Thus, we can integrate out the phonons in each domain wall and focus on the dynamics of the domain walls.

Integrating out the nearly perfectly reflecting phonons leads to two forces on the domain walls – a Casimir effect and phonon drag. The Casimir effect is generated by the standing waves formed by the phonons in each domain. To study the Casimir effect, we compute the “vacuum energy” due to the standing waves of long-wavelength phonons in a domain with length l , corresponding to

$$F_l = \frac{1}{\beta} \sum_{m=1}^{m_c} \ln(1 - e^{-\beta\omega_{k_m}}), \quad (7)$$

where β is the inverse temperature, $\omega_k = v_p k$ denotes the phonon frequency in the long-wavelength limit, v_p is the phonon velocity, $k_m = \pi m/l$ for the standing waves, and m_c is the number of long-wavelength phonons. In the low-temperature limit, the Casimir potential is approximated by:

$$V_{\text{Casimir}} \approx -TC \sum_n \ln \left[\frac{T}{\pi} (x_{n+1} - x_n) \right] + \text{const}, \quad (8)$$

where $\mathcal{C} = m_c$. The V_{Casimir} with a fixed number of domain walls is minimized when the domain walls are equal-spaced, i.e., domain sizes are the same. With the equipartition theorem, we obtain that the root-mean-square of domain-wall displacement is $\bar{l}/\sqrt{2\mathcal{C}}$, where \bar{l} is the averaged domain size. For sufficiently low (but nonzero) temperatures, \mathcal{C} is typically a large number. Thus, the domain wall fluctuation can be ignored.

Let us now discuss the origin of phonon drag which is a friction force that arises from the motion of the domain-wall relative to the phonons. Since domain walls strongly scatter off the long-wavelength phonons, the domain wall is also subject to a radiation pressure related to the flux of momentum $v_p \mathcal{E}$, where \mathcal{E} is the energy density of the phonons. The radiation pressure is balanced between the two sides at zero domain-wall velocity. At a finite velocity v of a domain wall, the longitudinal Doppler shift gives $\mathcal{E}'(v) = \mathcal{E} \sqrt{\frac{1-v/v_p}{1+v/v_p}}$ for phonons move in the same

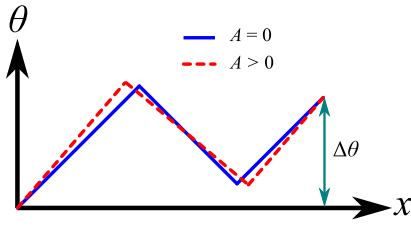


FIG. 3. Response to a uniform vector potential. In the presence of a uniform vector potential A , one can still find a solution satisfying the kinematic conditions and preserving the total variation of phase $\Delta\theta$.

direction as the domain wall. Thus, the phonons provide a drag force on the domain wall, described by

$$F_{\text{drag}} = v_p [\mathcal{E}(v) - \mathcal{E}(-v)] = -\gamma v, \quad (9)$$

where $\gamma \approx 2\mathcal{E}$ is the coupling constant of the phonon drag.

C. Mapping to classical problem

Following integrating out the phonon degrees of freedom, the long time-scale dynamics of the phase degree of freedom in Eq. 3 can be described in terms of the domain-wall coordinates, x_n and $\theta_n \equiv \theta(x_n)$ that keep tracks of the domain-wall position and phase respectively (see a discussion in Appendix C). Then, we map the imaginary-time action to a classical problem of $\hat{K} + \hat{V}$, where

$$\hat{K} = \int dx \frac{1}{2} (\partial_\tau \theta)^2 = \frac{1}{6} \sum_n (x_{n+1} - x_n) \left\{ \begin{array}{l} [\partial_\tau \theta_{n+1} - (\partial_\tau x_{n+1})(\partial_x \theta)]^2 \\ + [\partial_\tau \theta_{n+1} - (\partial_\tau x_{n+1})(\partial_x \theta)] [\partial_\tau \theta_n - (\partial_\tau x_n)(\partial_x \theta)] \\ + [\partial_\tau \theta_n - (\partial_\tau x_n)(\partial_x \theta)]^2 \end{array} \right\}, \quad (10)$$

$$\hat{V} = \int_x \left[-\frac{|r|}{2} (\partial_x \theta)^2 + \frac{1}{2} (\partial_x^2 \theta)^2 + u (\partial_x \theta)^4 \right] = \sum_n \int_n^{n+1} ds (x_{n+1} - x_n) \left\{ \frac{|r|}{4m_0^2} [(\partial_x \theta)^2 - m_0^2]^2 + \frac{1}{2} (\partial_x^2 \theta)^2 \right\}, \quad (11)$$

where s is an auxiliary variable such that $x(s) = (s-n)x_{n+1} + (n+1-s)x_n$ and $\theta(s) = (s-n)\theta_{n+1} + (n+1-s)\theta_n$. \hat{K} (\hat{V}) can be viewed as the “kinetic energy” (potential energy) of the classical problem. Since we are interested in the situation that the number of domain walls is fixed (i.e., ignoring the processes of annihilation or creation domain walls), we focus only on the contributions from the domains. The \hat{V} term is minimized when $(\partial_x \theta)^2 = m_0^2$ in each domain. Thus, we assume that

$$\partial_x \theta(x) = \frac{\theta_{n+1} - \theta_n}{x_{n+1} - x_n} = (-1)^{n+1} m_0, \quad (12)$$

for $x_n < x < x_{n+1}$. Using the Eqs. (10) and (12), we derive the zero-point kinetic energy term as follows

$$\begin{aligned} \hat{K}_0 = & \frac{1}{3} \sum_n (x_{2n+1} - x_{2n}) [\dot{a}_{2n+1}^2 + \dot{a}_{2n}^2 + \dot{a}_{2n+1} \dot{a}_{2n}] \\ & + \frac{1}{3} \sum_n (x_{2n} - x_{2n-1}) [\dot{b}_{2n}^2 + \dot{b}_{2n-1}^2 + \dot{b}_{2n} \dot{b}_{2n-1}] \end{aligned} \quad (13)$$

where x_n indicates the position of n th domain wall, $a_n = (\theta_n + m_0 x_n)/\sqrt{2}$, and $b_n = (\theta_n - m_0 x_n)/\sqrt{2}$ (see Fig. 2). The \hat{K}_0 term can be viewed as a collection of free particles with masses proportional to the domain sizes that vary in time.

D. Linear response theory

To quantify the slow dynamics of the domain-walls, we study the transport properties in the symmetry-broken regime. Transport in the condensate is determined by the response to a vector potential $A \geq 0$, equivalent to tilting the optical lattice in the experiments [2, 61]. The vector potential A and θ satisfy following gauge transformation: $A \rightarrow A + \partial_x \Lambda$ and $\theta \rightarrow \theta + \Lambda$. Therefore, we can incorporate the effect of vector potential by the minimal substitution: $\partial_x \theta \rightarrow \partial_x \theta - A$. In the presence of a uniform vector potential A , the minimal momentum becomes $m_0 + A$ and $-m_0 + A$, indicating that A modifies the slope in each domain. Assuming $0 < A < m_0$, one can easily find new configurations that follow the change of slopes in θ without changing the boundary phase $\Delta\theta$ as shown in Fig. 3. Intuitively, such a property implies the absence of response to a finite A , indicating a state with zero superfluid stiffness despite locally being a Bose condensate. In fact, the supercurrent (i.e., distortion of slope) due to an application of a vector potential can relax by dissipating energy into the phonon drag. The result is a finite relaxation time for the current that is similar to the decay of current following a transient electric field in an Ohmic conductor.

To confirm the absence of superfluid stiffness, we de-

velop a linear response theory for the symmetry-broken states and the Ohmic transport. The derivations are discussed in Appendix C, and we summarize the main ideas in the following. The goal is to derive the effective action of A by integrating out the the domain-wall variables, a_n and b_n . For simplicity, we assume a strong Casimir potential such that the domain walls are equally spaced and the domain size is \bar{l} . In the presence of A , we assume $\partial_x \theta = (-1)^{n+1} m_0 + h(x)$ for $x_n < x < x_{n+1}$, where $h(x)$ is a response to the applied vector potential A . In the imaginary-time path integral, we can derive $\mathcal{S}_V \approx \mathcal{S}_{A,0} + \mathcal{S}'_V$ [\mathcal{S}_V is associated with Eq. (11)], where

$$\mathcal{S}_{A,0} = \int d\tau dx |r| A^2, \quad (14)$$

$$\mathcal{S}'_V = \int d\tau \sum_n \left\{ \frac{2|r|}{t} \left[(a_{2n+1} - a_{2n})^2 + (b_{2n} - b_{2n-1})^2 \right] \right. \\ \left. - 2\sqrt{2}|r|A(a_{2n+1} - a_{2n} + b_{2n} - b_{2n-1}) \right\}. \quad (15)$$

In the above expression, we have expressed h in terms of the domain-wall variables and ignored $\partial_x h$ and $\partial_x A$ terms as we are interested in $k = 0$ limit. Together with \mathcal{S}_K [associated with Eq. (10)] and \mathcal{S}_{dis} [associated with Eq. (9)], the problem can be mapped to a normal-mode problem with complicated interactions. Then, we integrate out the domain-wall variables at the Gaussian level and derive an effective action for A as follows:

$$\mathcal{S}_{A,\text{eff}} \Big|_{k=0} \equiv \frac{\bar{l}}{\beta} \sum_{\omega_m} Q(\omega_m) \tilde{A}(-\omega_m) \tilde{A}(\omega_m).$$

The ac conductivity and superfluid stiffness can be obtained by $\sigma_{ac}(\omega) \propto \frac{i}{\omega} Q(\omega_m \rightarrow -i\omega - 0^+)$ and $\rho_s \propto Q(\omega_m = 0)$. When $\gamma \neq 0$, we obtain an Ohmic response in the real-part of low-frequency conductivity

$$\text{Re}[\sigma_{ac}(\omega)] \propto \frac{16m_0|r|^2\gamma(8m_0^2|r| + \gamma^2)\bar{l}}{(8m_0|r|\gamma)^2 + [(8m_0^2|r| + \gamma^2)\omega\bar{l}]^2}. \quad (16)$$

The superfluid stiffness ρ_s vanishes exactly, suggesting insulating behavior in a Bose condensate. Although the analytical results are derived with the equal-spaced domain wall assumption, the qualitative results remain the same for general situations. In Fig. 4(b), we provide numerical evidence showing the relaxation of current due to an applied vector potential, confirming our intuition and analytical calculations.

In continuous 1D systems, with momentum conservation, thermodynamic states can be associated with a certain momentum density. Such states, which result from the application of an electric field, carry a current even after the electric field is switched off. The resulting transport is effectively ballistic corresponding to infinite conductivity [62]. In our case with Z_2 symmetry-broken ground states, the momentum imparted to the system can be absorbed into changing the configuration of the domain-walls. Such a rearrangement transfers energy in the supercurrent into thermal energy of the phonons

through a drag force on the domain-walls. This dissipation of the current manifests as an ohmic response of the current to an electric field. Our theory shows a rare example of zero superfluid stiffness and Ohmic response in a continuous translation invariant 1D system. In this case, the domain walls can be thought of as playing a similar role to vortices in the high temperature phase of the 2D superfluid where the Lorentz force on vortices from an applied supercurrent results in a dissipative voltage.

E. Numerical results

To verify our theory numerically, we study bosons with a double-well dispersion using a discretized Gross-Pitaevski equation (GPE), which can simulate bosons in the semiclassical limit. First, we consider a lattice model given by

$$\hat{H}_{\text{Lat}} = -J_1 \sum_j (\psi_{j+1}^* \psi_j + h.c.) + J_2 \sum_j (\psi_{j+2}^* \psi_j + h.c.) \\ + \sum_j (\tilde{U} |\psi_j|^4 / 2 - \mu |\psi_j|^2), \quad (17)$$

where $J_1 > 0$ and $J_2 > 0$ denote the nearest neighbor and the second nearest neighbor hoppings respectively, and ψ_j is the bosonic annihilation operator at site j , and $\tilde{U} > 0$ is the onsite interaction. The kinetic energy term of the above Hamiltonian leads to a dispersion $\epsilon_k = -2J_1 \cos k + 2J_2 \cos 2k$, which yield two minima for $J_2/J_1 > 0.25$. We choose $J_2/J_1 = 0.4$ and $U/J_1 = 0.3$ for the parameters of our simulations. μ is chosen so that $\psi_j = 1$ is a ground state of the Hamiltonian. We then solve the Gross-Pitaevskii equations $i(d/dt)\psi_j = \delta \hat{H}_{\text{Lat}} / \delta \psi_j^*$ numerical using the *ode89* solver in MATLAB from the various initial conditions that we discuss below.

The main goal of our simulation is to confirm the non-superfluid Ohmic response of the finite temperature state with a few domain-walls. To do this, we choose initial conditions $\psi_j = e^{i\theta_j}$ together with a choice for the phase-variable θ_j where the sign of the slope of θ_j varies across domain-walls in space. In addition, we assume that the system is subject to a large uniform electric field for a short time, which as discussed in the context of Fig. 3, corresponds to a tilting of the phase profile $\theta_j \rightarrow \theta_j + A_j$. The ensuing dynamics obtained from the numerical solution of the GPE, shown in Fig. 4(a), confirms the relaxation of the phase profile to a configuration where the slopes obey the ground state value as time progress through the simulation.

To understand the observable transport consequences of this relaxation we compute the discrete current operator

$$I_j = -J_1 \text{Im}[\psi_{2j+1}^* \psi_{2j}] + J_2 \text{Im}[\psi_{2j}^* \psi_{2j-2} + \psi_{2j+1}^* \psi_{2j-1}]. \quad (18)$$

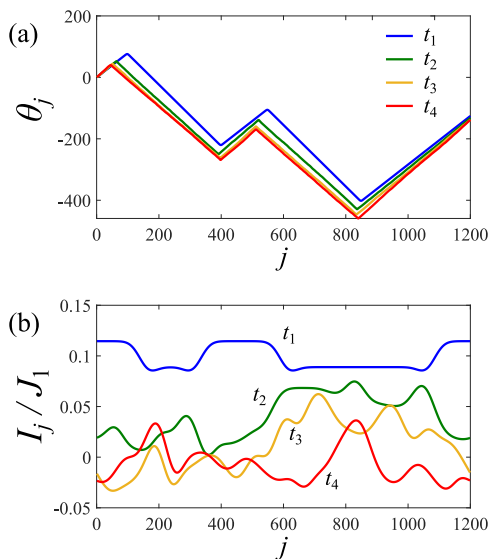


FIG. 4. Numerical results for time evolution of phase and current profiles. We first prepare an initial stationary state and then insert a vector potential $A = 40\pi/L$ with $L = 1200$ at $t = 0$. (a) The phase configurations with different times. (b) The current configurations with different times. $t_1 = 2/J_1$, $t_2 = 4860/J_1$, $t_3 = 7290/J_1$, and $t_4 = 9720/J_1$. The numerical results are obtained by solving Gross-Pitaevskii equation with the *ode89* solver in MATLAB.

This current operator corresponds to a ladder configuration where the sites are paired up into dimers ($2j-1, 2j$) and the current I_j is between neighboring dimers. The simulated current profiles corresponding to the phase profiles in Fig. 4(a) are shown in Fig. 4(b). The results for the current profiles (after smoothening to eliminate short-wavelength phonons) show that the average current decreases from nearly $I_{av} \sim 0.1J_1$ to $I_{av} \sim 0$. The decay of the currents confirms the non-superfluid ohmic charge transport.

IV. LIFSHITZ QUANTUM HYDRODYNAMICS NEAR QUANTUM CRITICALITY

So far, we have focused on the dynamics in the symmetry-broken phase supporting multiple domains. It is also interesting to study the dynamics near the quantum criticality point. The quantum Lifshitz theory [i.e., Eq. (3) with $r = u = 0$] is at an unstable fixed point, and the renormalization group (RG) flows lead to an interacting fixed point with $r < 0$ and $u > 0$ [63, 64]. Thus, we focus on the dynamics in the vicinity of the interacting fixed point.

First, we construct the currents (j_x, j_t) and stress tensors ($T_{xx}, T_{xt}, T_{tx}, T_{tt}$) using Euler-Lagrangian equation (see Appendix D for a discussion). The conservation

laws are expressed by:

$$\partial_t j_t + \partial_x j_x = 0, \quad (19a)$$

$$\partial_t T_{xt} + \partial_x T_{xx} = 0, \quad (19b)$$

$$\partial_t T_{tt} + \partial_x T_{tx} = 0, \quad (19c)$$

corresponding to conservation of particle number ($N = \int dx j_t$), momentum ($P = \int dx T_{xt}$), and energy ($E = \int dx T_{tt}$), respectively. Then, we construct a free energy, $F[s, \mu, \beta, v]$, defined by

$$e^{-\beta F[s, \mu, \beta, v]} = \text{Tr} \left[e^{-\beta \int dx (s T_{tt} - v T_{xt} - \mu j_t)} \right], \quad (20)$$

where $\beta = 1/T$ is the inverse temperature, s is a dimensionless parameter (s is set to 1 at the end of calculations), v is the center of mass velocity, μ is the chemical potential. Using hyperscaling, we derive that

$$\frac{F[s, \mu, 1/T, v]}{L} = T^{1+\frac{d}{z}} \Phi \left[s, \frac{\mu}{T^{\frac{y_\mu}{z}}}, \frac{v}{T^{\frac{y_v}{z}}} \right], \quad (21)$$

where Φ is a universal scaling function, y_μ and y_v are the RG eigenvalue of μ and v , respectively. The variation of currents and stress tensors can be generally expressed by

$$\delta \langle j_t \rangle = \chi_\mu \delta \mu + \chi_\beta \delta \beta, \quad (22a)$$

$$\delta \langle j_x \rangle = \rho_N \delta v, \quad (22b)$$

$$\delta \langle T_{xx} \rangle = K_\beta \delta \beta + K_\mu \delta \mu, \quad (22c)$$

$$\delta \langle T_{xt} \rangle = \rho_M \delta v, \quad (22d)$$

$$\delta \langle T_{tx} \rangle = \rho_E \delta v, \quad (22e)$$

$$\delta \langle T_{tt} \rangle = C_\beta \delta \beta + C_\mu \delta \mu, \quad (22f)$$

where C_β and C_μ are specific heats, K_β and K_μ are the bulk moduli, and χ_β and χ_μ are the compressibilities. The finite-temperature scaling of the above quantities can be derived easily combined with RG analysis [63, 64]. In particular, $\rho_M \sim T^{-1}$ corresponds to diverging inertia at zero temperature. Concomitantly, the superfluid stiffness $\rho_s \sim \rho_M^{-1} \sim T$, vanishes at zero temperature. It is worth mentioning that the classical gases with Lifshitz dispersion yield a different finite-temperature scaling in the inertia, $\rho_M \sim T^{-1/2}$. See Appendix D for a discussion.

Using Eq. (22), the conservation laws [Eq. (19)], $\partial_a \langle T_{ba} \rangle = 0$ and $\partial_a \langle j_a \rangle = 0$ can be expressed by a matrix equation [65, 66]. We further express $\delta \mu$, δv , and $\delta \beta$ in terms of $\delta \langle T_{tt} \rangle$, $\delta \langle T_{xt} \rangle$, and $\delta \langle j_t \rangle$. Finally, we derive a wave equation given by

$$\partial_t \begin{bmatrix} \epsilon \\ p \\ n \end{bmatrix} = \begin{bmatrix} 0 & M_4 & 0 \\ M_3 & 0 & M_2 \\ 0 & M_1 & 0 \end{bmatrix} \partial_x \begin{bmatrix} \epsilon \\ p \\ n \end{bmatrix}, \quad (23)$$

where $\epsilon = \langle T_{tt} \rangle$ is the energy density, $p = \langle T_{xt} \rangle$ is the momentum density, $n = \langle j_t \rangle$ is the number density, $M_1 = \rho_N / \rho_M$, $M_2 = \frac{C_\mu K_\beta - C_\beta K_\mu}{C_\mu \chi_\beta - C_\beta \chi_\mu}$, $M_3 = \frac{K_\mu \chi_\beta - K_\beta \chi_\mu}{C_\mu \chi_\beta - C_\beta \chi_\mu}$, $M_4 =$

ρ_E/ρ_M . The eigenvalues of the matrix in Eq. (D44) correspond to the sound velocities, which are given by $v = 0, \pm v_s$, where $v_s = \sqrt{M_1 M_2 + M_3 M_4}$.

The expression of sound velocity can be derived through the susceptibilities and response functions. Since we are primarily interested in the dynamics controlled by the interacting fixed point, we adopt the results based on RG scalings [63, 64]. We find that $M_1 \sim T$, $M_2 \sim T^0$, $M_3 \sim T^{-3/4}$, and $M_4 \sim T^{7/4}$. Thus, the sound velocity $v_s \sim T^{1/2}$, which vanishes at zero temperature. We also note that the scaling of the Gaussian fixed point (i.e., $r = u = 0$) yields the same results as discussed in Appendix D. At zero temperature, the absence of superfluid stiffness and sound velocity imply that the dynamics in the quantum critical regime is very slow, qualitatively similar to the symmetry-broken regime.

V. DISCUSSION

We demonstrate unconventional constrained domain-wall dynamics in the symmetry-broken phase of 1D superfluid with double-well dispersion. The relaxation is unexpectedly slow, the superfluid stiffness $\rho_s = 0$, and the transport response is Ohmic-like. Ohmic transport in one dimension necessarily requires relaxation of momenta. This is reminiscent of how a free vortex gas in 2D superfluids can lead to ohmic transport in the absence of impurities. The slowly moving domain walls strongly coupled to phonons are the unique features of the current system that makes this possible. These unusual results reveal slow dynamics in the symmetry-broken regime. We also find that superfluid stiffness $\rho_s \sim T$ and sound velocity $v_s \sim T^{1/2}$ in the vicinity of the quantum critical point, showing the incipient of slow dynamics. Moreover, our theory provides a natural explanation of the long-lived domain walls observed in experiments [10, 12], and the condensates with robust domain walls are promising to preserve information under unwanted perturbations.

In the low-temperature symmetry-broken regime, the constrained domain-wall motion results in an unusual slow dynamics. To see this, we first discuss the transverse-field Ising model (TFIM) in the symmetry-broken regime [67, 68], where the spin-spin correlation can be computed within semi-classical treatment. We can estimate the correlation time τ_{TFIM}^{-1} using $\tau_{\text{TFIM}}^{-1} \sim v_T \xi_c^{-1}$, where $v_T \sim c\sqrt{T/\Delta}$ is the thermal velocity obtained from equipartition theorem, c is the velocity of the excitation, Δ is the energy cost of domain wall, $\xi_c = l_0/2$ is the correlation length, and $l_0 \sim e^{\Delta/T}$ is the mean domain size (upto power-law correction in T). The correlation time estimated this way only differs from the exact result [67, 68] by an overall numerical prefactor. In our case, the primary relaxation is the collective domain motion (with a mass proportional to the domain size), and the phonon fluctuation induces a diffusive motion for the center of mass of domain. Thus, we obtain the momentum-momentum autocorrelation func-

tion $\langle \partial_x \theta(x, t) \partial_x \theta(x, 0) \rangle \propto \exp(-|t|/\tau_{\text{DW}})$ upto subleading power-law corrections, where $\tau_{\text{DW}} \propto l_0^2 \sim e^{2\Delta/T}$. (See Appendix E) for a discussion. Note that the correlation time τ_{DW} is significant larger than the $\tau_{\text{TFIM}} \propto l_0 \sim e^{\Delta/T}$. (We drop the power-law correction in T because the exponential term dominates at low temperatures.) For completeness, we discuss the $\gamma = 0$ case where domains move ballistically. Using the similar analysis for TFIM, we obtain $\tau'_{\text{DW}} \propto l_0^{3/2} \sim e^{3\Delta/(2T)}$ which is an intermediate value between τ_{DW} and τ_{TFIM} .

The conservation of dipole moment in our model is analogous but also distinct to the S_z conservation in several spin-1/2 models [69, 70] that demonstrate Hilbert space fragmentation [69–78]. Both conservation laws lead to slow dynamics – however, the dipole moment is associated with defects rather than each point of the system. Furthermore, the dynamics of these S_z -conserving systems occur in a closed system without the need for an external bath. In our case, The phonons serve as the bath of the system. In the low-temperature regime, we can consider the Hilbert space fragmentation for our system of bosons with a double-well dispersion. The connection to Hilbert space fragmentation provides a natural intrinsic explanation for the slow dynamics of 1D bosons with double-well dispersion in the absence of spatial inhomogeneity or integrability. The fragmented subspaces in Hilbert space remain disconnected under time evolution, resulting in an out-of-equilibrium asymptotic state. In our case, the phonons will cause true thermalization in the infinite time limit, but the effective Hilbert space fragmentation still manifests on a prethermalization time scale (relevant to the time scale in the AMO experiments), similar to the slow relaxation of quantum systems with dynamical constraints [79].

The constrained dynamics due to the dipole moment conservation in the symmetry-broken regime suggests a connection to the fractonic systems [38–57]. In the vicinity of the quantum critical point [63, 64], the scaling results are the same as the $(1+1)D$ quantum Lifshitz theory, which also suggests a potential connection to fractions through the quantum Lifshitz theory [53, 54, 56]. In particular, the superfluid stiffness vanishes to zero at $T = 0$ in the symmetry-broken and the quantum critical regime, qualitatively consistent with the zero superfluid stiffness in the symmetry-broken regime. However, we note that there are several terms, which we omitted, may complicate the potential connection between the quantum critical regime and the quantum Lifshitz field theory. For example, the $i\partial_\tau(\partial_x \theta)^2$ term can induce a fluctuation-driven first order transition [80], sabotaging the present scaling analysis. The ignorance of additional terms does not affect any of our qualitative results in the symmetry-broken regime, but it limits the scaling analysis to a finite temperature distant away from the quantum critical point.

In this work, we focus only on $\delta \gg 1$ and ignore the fluctuation in density. We anticipate similar constrained domain-wall motion in the general cases, includ-

ing $\delta \ll 1$ (requiring both density and phase fields). The main difference is that the domain walls in the $\delta \ll 1$ regime feature inevitable density fluctuations (related to the phase staircases) [29]. Much of our analysis based on long-wavelength theory still applies, e.g., long-wavelength phonons are confined in each domain and phonon drag. Therefore, we argue that the superfluid with double-well dispersion generically manifests robust domain walls and slow dynamics in the symmetry-broken regime.

ACKNOWLEDGMENTS

Acknowledgments.— We thank Maissam Barkeshli, Cheng Chin, Matthew Foster, Andrey Gromov, Han Pu, Chunlei Qu, Krishnendu Sengupta, and Zhi-Cheng Yang for useful discussions. This work is supported by the Laboratory for Physical Sciences, by JQI-NSF-PFC (Y.-Z.C.), by ARO W911NF2010232 (Y.-Z.C.), and by NSF DMR – 1555135 (J.D.S.).

Appendix A: Derivation of effective action

We consider 1D complex bosons described by

$$\mathcal{S} = \int_{\tau,x} [b^* \partial_\tau b - B |\partial_x b|^2 + C |\partial_x^2 b|^2 + U |b|^4 - \mu |b|^2], \quad (\text{A1})$$

where b is the complex boson field. We require $C > 0$ for the stability of the theory. When $B < 0$, the dispersion of the boson can be approximated by the conventional k^2 dispersion (upto a k^4 correction). When $B > 0$, the dispersion of the boson is a double-well. $B = 0$ is the Lifshitz point.

In the high density limit, we use a density-phase representation for the boson field,

$$b(\tau, x) \approx \sqrt{n(\tau, x)} e^{i\phi(\tau, x)}. \quad (\text{A2})$$

We can express the derivatives of b as follows:

$$b^* \partial_\tau b \rightarrow \frac{1}{2} \partial_\tau n + n (i \partial_\tau \phi), \quad (\text{A3})$$

$$\partial_x b \rightarrow \frac{1}{2} \frac{(\partial_x n)}{n} b + b (i \partial_x \phi), \quad (\text{A4})$$

$$|\partial_x b|^2 \rightarrow \frac{1}{4} \frac{(\partial_x n)^2}{n} + n (\partial_x \phi)^2, \quad (\text{A5})$$

$$\partial_x^2 b \rightarrow \frac{1}{2} \frac{(\partial_x^2 n)}{n} b - \frac{1}{4} \frac{(\partial_x n)^2}{n^2} b - b (\partial_x \phi)^2 + i \left[\frac{\partial_x n}{n} (\partial_x \phi) b + b (\partial_x^2 \phi) \right] \quad (\text{A6})$$

$$\begin{aligned} |\partial_x^2 b|^2 &\rightarrow \frac{1}{4} \frac{(\partial_x^2 n)^2}{n} + \frac{1}{16} \frac{(\partial_x n)^4}{n^3} + n (\partial_x \phi)^4 - \frac{1}{4} \frac{(\partial_x^2 n) (\partial_x n)^2}{n^2} - (\partial_x^2 n) (\partial_x \phi)^2 \\ &\quad + \frac{1}{2} \frac{(\partial_x n)^2}{n} (\partial_x \phi)^2 + \frac{(\partial_x n)^2}{n} (\partial_x \phi)^2 + n (\partial_x^2 \phi)^2 + 2 (\partial_x^2 \phi) (\partial_x \phi) (\partial_x n) \end{aligned} \quad (\text{A7})$$

The action given by Eq. (A1) becomes to

$$\mathcal{S} \rightarrow \int_{\tau,x} \left\{ \begin{aligned} &\frac{1}{2} \partial_\tau n + n (i \partial_\tau \phi) - B n (\partial_x \phi)^2 + U n^2 - \mu n \\ &+ C \left[n (\partial_x^2 \phi)^2 + n (\partial_x \phi)^4 - (\partial_x^2 n) (\partial_x \phi)^2 + 2 (\partial_x^2 \phi) (\partial_x \phi) (\partial_x n) \right] \\ &- B \frac{1}{4} \frac{(\partial_x n)^2}{n} + C \left[\frac{1}{4} \frac{(\partial_x^2 n)^2}{n} + \frac{1}{16} \frac{(\partial_x n)^4}{n^3} - \frac{1}{4} \frac{(\partial_x^2 n) (\partial_x n)^2}{n^2} + \frac{3}{2} \frac{(\partial_x n)^2}{n} (\partial_x \phi)^2 \right] \end{aligned} \right\}. \quad (\text{A8})$$

We assume that $n(\tau, x) = n_0 + \delta n(\tau, x)$, where n_0 is the uniform background density and δn is the fluctuation. By

minimizing the free energy, one find that $n_0 = \mu/(2U)$. When $\delta n \ll n_0$, the action [given by Eq. (A8)] becomes to

$$\mathcal{S} \rightarrow \int_{\tau,x} \left\{ \begin{aligned} & \frac{1}{2}(\partial_\tau \delta n) + (n_0 + \delta n) (i\partial_\tau \phi) - B(n_0 + \delta n) (\partial_x \phi)^2 + U(n_0 + \delta n)^2 - \mu(n_0 + \delta n) \\ & + C \left[(n_0 + \delta n) (\partial_x^2 \phi)^2 + (n_0 + \delta n) (\partial_x \phi)^4 - (\partial_x^2 \delta n) (\partial_x \phi)^2 + 2 (\partial_x^2 \phi) (\partial_x \phi) (\partial_x \delta n) \right] \\ & - B \frac{1}{4} \frac{(\partial_x \delta n)^2}{(n_0 + \delta n)} + C \left[\frac{1}{4} \frac{(\partial_x^2 \delta n)^2}{(n_0 + \delta n)} + \frac{1}{16} \frac{(\partial_x \delta n)^4}{(n_0 + \delta n)^3} - \frac{1}{4} \frac{(\partial_x^2 \delta n)(\partial_x \delta n)^2}{(n_0 + \delta n)^2} + \frac{3}{2} \frac{(\partial_x \delta n)^2}{(n_0 + \delta n)} (\partial_x \phi)^2 \right] \end{aligned} \right\} \quad (\text{A9})$$

$$= \int_{\tau,x} \left\{ \begin{aligned} & \frac{1}{2}(\partial_\tau \delta n) + in_0(\partial_\tau \phi) \\ & + U(\delta n)^2 + 2Un_0\delta n + Un_0^2 - \mu\delta n - \mu n_0 - B\frac{1}{4}\frac{(\partial_x \delta n)^2}{n_0} + C\frac{1}{4}\frac{(\partial_x^2 \delta n)^2}{n_0} + \dots \\ & - Bn_0(\partial_x \phi)^2 + Cn_0(\partial_x^2 \phi)^2 + Cn_0(\partial_x \phi)^4 \\ & + i\delta n(\partial_\tau \phi) - B\delta n(\partial_x \phi)^2 + C\delta n(\partial_x^2 \phi)^2 + C\delta n(\partial_x \phi)^4 - 2C(\partial_x^2 \delta n)(\partial_x \phi)^2 + C\frac{3}{2}\frac{(\partial_x \delta n)^2}{n_0}(\partial_x \phi)^2 + \dots \end{aligned} \right\} \quad (\text{A10})$$

$$= \int_{\tau,x} \left\{ \begin{aligned} & +U \left[(\delta n)^2 - \frac{B}{2\mu} (\partial_x \delta n)^2 + \frac{C}{2\mu} (\partial_x^2 \delta n)^2 \right] + \dots \\ & + \frac{\mu}{2U} \left[-B(\partial_x \phi)^2 + C(\partial_x^2 \phi)^2 + C(\partial_x \phi)^4 \right] \\ & + i\delta n(\partial_\tau \phi) - B\delta n(\partial_x \phi)^2 + C\delta n(\partial_x^2 \phi)^2 + C\delta n(\partial_x \phi)^4 - 2C(\partial_x^2 \delta n)(\partial_x \phi)^2 + \frac{3CU}{\mu} (\partial_x \delta n)^2 (\partial_x \phi)^2 + \dots \end{aligned} \right\}. \quad (\text{A11})$$

In the last equation, $n_0 = \mu/(2U)$ is used. The total derivative terms as well as the higher order in $\delta n/n_0$ terms are dropped.

(density-phase couplings). These actions are given by

$$\mathcal{S}_n = U \int_{\tau,x} \left[(\delta n)^2 - \frac{B}{2\mu} (\partial_x \delta n)^2 + \frac{C}{2\mu} (\partial_x^2 \delta n)^2 \right], \quad (\text{A12})$$

$$\mathcal{S}_\phi = \frac{\mu}{2U} \int_{\tau,x} \left[-B(\partial_x \phi)^2 + C(\partial_x^2 \phi)^2 + C(\partial_x \phi)^4 \right], \quad (\text{A13})$$

$$\mathcal{S}_c \approx \int_{\tau,x} \delta n \left[i(\partial_\tau \phi) - B(\partial_x \phi)^2 + C(\partial_x^2 \phi)^2 + C(\partial_x \phi)^4 \right], \quad (\text{A14})$$

where we have dropped a few more irrelevant terms in \mathcal{S}_c . The density fluctuation is controlled by U while the phase fluctuation is controlled by $n_0 = \mu/(2U)$.

Formally, one can integrate out the density fluctuation at the Gaussian level and construct an effective action of the phase mode. The effective action is given by

The action \mathcal{S} can be decomposed into three parts: \mathcal{S}_n (density fluctuation), \mathcal{S}_ϕ (phase fluctaiton), and \mathcal{S}_c

$$\mathcal{S}_{\text{eff}} = \frac{\mu}{2U} \int_{\tau,x} \left[-B(\partial_x \phi)^2 + C(\partial_x^2 \phi)^2 + C(\partial_x \phi)^4 \right] - \frac{1}{U} \int_{\tau,x} \frac{\left[i(\partial_\tau \phi) - B(\partial_x \phi)^2 + C(\partial_x^2 \phi)^2 + C(\partial_x \phi)^4 \right]^2}{1 + \frac{B}{2\mu} \partial_x^2 + \frac{C}{2\mu} \partial_x^4} \quad (\text{A15})$$

$$\approx \frac{\mu}{2U} \int_{\tau,x} \left[-B(\partial_x \phi)^2 + C(\partial_x^2 \phi)^2 + C(\partial_x \phi)^4 \right] + \int_{\tau,x} \left[\frac{1}{U} (\partial_\tau \phi)^2 + 2i\frac{B}{U} (\partial_\tau \phi) (\partial_x \phi)^2 + \frac{B}{2\mu U} (\partial_\tau \partial_x \phi)^2 - \frac{B^2}{U} (\partial_x \phi)^4 \right] \quad (\text{A16})$$

$$= \frac{\mu}{2U} \int_{\tau,x} \left[\frac{2}{\mu} (\partial_\tau \phi)^2 + i\frac{4B}{\mu} (\partial_\tau \phi) (\partial_x \phi)^2 + \frac{B}{\mu^2} (\partial_\tau \partial_x \phi)^2 - B(\partial_x \phi)^2 + C(\partial_x^2 \phi)^2 + \left(C - \frac{2B^2}{\mu} \right) (\partial_x \phi)^4 \right]. \quad (\text{A17})$$

The above effective action has a few interesting proper-

ties. First of all, the $i(\partial_\tau \phi)(\partial_x \phi)^2$ appears. This term

is believed to drive the phase transition to a first order transition. Otherwise, higher order terms are required. The $(\partial_\tau \partial_x \phi)^2$ corresponds to the dynamical term of the gauge field. The stability of the effective theory is set by $C - \frac{2B^2}{\mu} > 0$, and the value of optimal momentum $k^* = \partial_x \phi$ becomes $\pm \sqrt{\frac{B}{2C - 4B^2/\mu}}$, which recovers the non-interacting value $\pm \sqrt{\frac{B}{2C}}$ when $\mu \rightarrow \infty$. The renormalized value of k^* is a manifestation of interaction effect.

To simplify the effective action, we introduce rescaling parameters, $\theta = \mathcal{A}^{-1} \phi$ and $\tilde{\tau} = \mathcal{B}^{-1} \tau$, where $\mathcal{A} = (\frac{2}{\mu C})^{1/4} U^{1/2}$ and $\mathcal{B} = (2\mu C)^{-1/2}$. Thus, the effective action given by Eq. (A17) becomes

$$S_{\text{eff}} = \int_{\tilde{\tau}, x} \left[\frac{1}{2} (\partial_{\tilde{\tau}} \theta)^2 + i\zeta (\partial_{\tilde{\tau}} \theta) (\partial_x \theta)^2 + \frac{g}{2} (\partial_{\tilde{\tau}} \partial_x \theta)^2 + \frac{r}{2} (\partial_x \theta)^2 + \frac{1}{2} (\partial_x^2 \theta)^2 + u (\partial_x \theta)^4 \right], \quad (\text{A18})$$

where ζ, g, r, u are the rescaled parameters. In the main text, we drop ζ and g terms. We also make a notational substitution $\tilde{\tau} \rightarrow \tau$ for the simplicity of presentation.

Appendix B: Scattering problem at a domain wall

As we discussed in main text, a single-domain-wall solution can be described by

$$\theta_{\text{DW}}(x) = \theta_0 + m_0 \sqrt{\frac{2}{|r|}} \ln \left[\cosh \left(\sqrt{\frac{|r|}{2}} x \right) \right], \quad (\text{B1})$$

where we have set the domain-wall position at $x = 0$. The (real-time) equation of motion is given by

$$\partial_t (\partial_t \theta) - \partial_x \left[r (\partial_x \theta) + 4u (\partial_x \theta)^3 - \partial_x^3 \theta \right] = 0. \quad (\text{B2})$$

Now, we substitute θ by $\theta_{\text{DW}}(x) + \delta\theta(t, x)$ and rewrite the equation of motion as follows:

$$\partial_t^2 \delta\theta - \partial_x \left[\begin{array}{l} -|r| (\partial_x \delta\theta) + 12u (\partial_x \theta_{\text{DW}})^2 (\partial_x \delta\theta) \\ + 12u (\partial_x \theta_{\text{DW}}) (\partial_x \delta\theta)^2 \\ + 4u (\partial_x \delta\theta)^3 - (\partial_x^3 \delta\theta) \end{array} \right] = 0, \quad (\text{B3})$$

where we have used the fact that θ_{DW} obeys the equation of motion. For $\sqrt{|r|/2}|x| \gg 1$, we can derive the linearized equation of motion (ignoring $O(\delta\theta^2)$) as follows

$$\begin{aligned} \partial_t^2 \delta\theta - \partial_x \left[-|r| (\partial_x \delta\theta) + 12um_0^2 (\partial_x \delta\theta) - (\partial_x^3 \delta\theta) \right] &= 0 \\ \rightarrow \left[\partial_t^2 - 2|r| \partial_x^2 + \partial_x^4 \right] \delta\theta &= 0, \end{aligned} \quad (\text{B4})$$

where we have used $m_0^2 = |r|/(4u)$. The above wave equation gives the dispersion of the phonon in the linearized regime. In the long-wavelength limit, we obtain $\omega^2 = v_p^2 k^2$, where $v_p = \sqrt{2|r|}$.

The general scattering problem can be solved by studying Eq. (B3). Here, we focus only on the long-wavelength limit. Since the problem has a reflection symmetry about $x = 0$, we can rewrite $\delta\theta$ as $\delta\theta = a_S \theta_S + a_A \theta_A$, where

$$\theta_S(x)|_{|x| \rightarrow \infty} = \cos(k|x| + \alpha_{S,k}), \quad (\text{B5})$$

$$\theta_A(x)|_{|x| \rightarrow \infty} = \cos(k|x| + \alpha_{A,k}) \text{sgn}(x). \quad (\text{B6})$$

In the above expression, $\alpha_{S,k}$ and $\alpha_{A,k}$ are the phase factors. We can show that there are two zero modes ($\omega \rightarrow 0$) of the equation of motion in Eq. (B2): (a) An overall constant shift in θ and (b) domain-wall translation. Thus, one can easily show that $\alpha_{S,k} = 0$ and $\alpha_{A,k} = 0$ for $k \rightarrow 0$. Then, we consider the conventional scattering waves far away from the domain wall ($x = 0$),

$$\delta\theta(x)|_{x \rightarrow -\infty} \propto e^{ikx} + a_R e^{-ikx}, \quad (\text{B7})$$

$$\delta\theta(x)|_{x \rightarrow \infty} \propto a_t e^{ikx}. \quad (\text{B8})$$

We can easily show find that $a_S = -a_A$ satisfy the scattering ansatz with $a_r = 1$ and $a_t = 0$, corresponding to the perfect reflection at the domain wall. Therefore, we expect that the long-wavelength phonons form standing waves in each domain.

Appendix C: Classical model for domain wall dynamics

In this section, we present a framework for studying the response to a vector potential in a symmetry-broken state with multiple domains. We first introduce the collective variables and the Lagrangian coordinates. Then, we develop a linear-response theory and compute the response function.

1. Collective coordinate

To describe the motion of domains, we introduce a set of collective variables as follows:

$$a(x) = \frac{1}{\sqrt{2}} [\theta(x) + m_0 x], \quad b(x) = \frac{1}{\sqrt{2}} [\theta(x) - m_0 x]. \quad (\text{C1})$$

Conversely,

$$\theta(x) = \frac{1}{\sqrt{2}} [a(x) + b(x)], \quad x = \frac{1}{\sqrt{2}m_0} [a(x) - b(x)]. \quad (\text{C2})$$

We can express $(x, \theta(x))$ in terms of (a, b) .

2. General formalism for domain-wall dynamics

We construct a general formalism for studying the domain wall dynamics in this subsection. To keep track of

the domain walls, we introduce a Lagrangian coordinate s , and the Eulerian coordinate $x \equiv X(\tau, s)$. Formally, we can also view this as a reparametrization from (τ, x) to (τ, s) . We require that s_n labels the n th domain with position $X(\tau, s_n)$. Without loss of generality, we set $s_n = n$. Note that x without specifying s is just a variable, i.e., independent of τ . The τ -dependence is acquired when the value of s is assigned. The total derivative of X is expressed by

$$dx = \left(\frac{\partial X}{\partial \tau} \right)_s d\tau + \left(\frac{\partial X}{\partial s} \right)_\tau ds, \quad (\text{C3})$$

where the subscript τ (s) in the partial derivative means fixing τ (s). We derive two useful identities

$$\frac{dx}{dx} = 1 = \left(\frac{\partial X}{\partial \tau} \right)_s \frac{d\tau}{dx} + \left(\frac{\partial X}{\partial s} \right)_\tau \frac{ds}{dx} \rightarrow dx = \left(\frac{\partial X}{\partial s} \right)_\tau ds \quad (\text{C4})$$

$$\frac{dx}{d\tau} = 0 = \left(\frac{\partial X}{\partial \tau} \right)_s + \left(\frac{\partial X}{\partial s} \right)_\tau \frac{ds}{d\tau} \rightarrow \frac{ds}{d\tau} = - \left(\frac{\partial X}{\partial s} \right)_\tau \quad (\text{C5})$$

We also define $\theta \equiv \tilde{\theta}(\tau, s)$. The derivatives of θ are given by

$$\partial_x \theta = \frac{\left(\frac{\partial \tilde{\theta}}{\partial s} \right)_\tau}{\left(\frac{\partial X}{\partial s} \right)_\tau}, \quad (\text{C6})$$

$$\partial_\tau \theta = \left(\frac{\partial \tilde{\theta}}{\partial \tau} \right)_s + \left(\frac{\partial \tilde{\theta}}{\partial s} \right)_\tau \frac{ds}{d\tau}, \quad (\text{C7})$$

We consider a state such that

$$\tilde{\theta}(\tau, s) = (s - n)\theta_{n+1} + (n + 1 - s)\theta_n, \quad (\text{C8a})$$

$$X(\tau, s) = (s - n)x_{n+1} + (n + 1 - s)x_n, \quad (\text{C8b})$$

for $n \leq s \leq n + 1$. In the above expression, $x_n \equiv X|_{s=n}$ and $\theta_n \equiv \tilde{\theta}|_{s=n}$ correspond to position and the phase variable of the n th domain wall. We note that Eq. (C8) does not incorporate the accurate shape of domain walls. Based on Eq. (C8), we compute

$$\partial_x \theta = \frac{\theta_{n+1} - \theta_n}{x_{n+1} - x_n}, \quad (\text{C9})$$

$$\partial_\tau \theta = (s - n) [\partial_\tau \theta_{n+1} - (\partial_\tau x_{n+1})(\partial_x \theta)] - (n + 1 - s) [\partial_\tau \theta_n - (\partial_\tau x_n)(\partial_x \theta)], \quad (\text{C10})$$

for $n < s < n + 1$.

Our goal is to study the symmetry-broken state with multiple domains. In the imaginary-time formalism, we can treat the problem as a classical string described by an effective Hamiltonian $H_{\text{eff}} = K + V$, where

$$K = \int_x \frac{1}{2} (\partial_\tau \theta)^2 = \frac{1}{2} \sum_n \int_n^{n+1} ds (x_{n+1} - x_n) \left\{ \begin{array}{l} (s - n)^2 [\partial_\tau \theta_{n+1} - (\partial_\tau x_{n+1})(\partial_x \theta)]^2 \\ + 2(s - n)(n + 1 - s) [\partial_\tau \theta_{n+1} - (\partial_\tau x_{n+1})(\partial_x \theta)] [\partial_\tau \theta_n - (\partial_\tau x_n)(\partial_x \theta)] \\ + (n + 1 - s)^2 [\partial_\tau \theta_n - (\partial_\tau x_n)(\partial_x \theta)]^2 \end{array} \right\} \\ = \frac{1}{6} \sum_n (x_{n+1} - x_n) \left\{ \begin{array}{l} [\partial_\tau \theta_{n+1} - (\partial_\tau x_{n+1})(\partial_x \theta)]^2 \\ + [\partial_\tau \theta_{n+1} - (\partial_\tau x_{n+1})(\partial_x \theta)] [\partial_\tau \theta_n - (\partial_\tau x_n)(\partial_x \theta)] \\ + [\partial_\tau \theta_n - (\partial_\tau x_n)(\partial_x \theta)]^2 \end{array} \right\}, \quad (\text{C11})$$

$$V = \int_x \left[-\frac{|r|}{2} (\partial_x \theta)^2 + \frac{1}{2} (\partial_x^2 \theta)^2 + \frac{|r|}{4m_0^2} (\partial_x \theta)^4 \right] = \sum_n \int_n^{n+1} ds (x_{n+1} - x_n) \left\{ \frac{|r|}{4m_0^2} [(\partial_x \theta)^2 - m_0^2]^2 + \frac{1}{2} (\partial_x^2 \theta)^2 \right\}. \quad (\text{C12})$$

To derive the zero-point kinetic energy, we assume that $\partial_x \theta = (-1)^{n+1} m_0$ for $n < s < n + 1$. Moreover, we ignore the $(\partial_x^2 \theta)^2$ term in V as it give rise to the domain wall

energy, which we assume to be a constant for our fixed domain wall number calculations. Thus, the zero-point kinetic energy is expressed by

$$\begin{aligned}
K_0 &= \frac{1}{6} \sum_n (x_{n+1} - x_n) \left\{ + \frac{[\partial_\tau \theta_{n+1} - (\partial_\tau x_{n+1})(-1)^{n+1} m_0]^2}{[\partial_\tau \theta_{n+1} - (\partial_\tau x_{n+1})(-1)^{n+1} m_0] [\partial_\tau \theta_n - (\partial_\tau x_n)(-1)^{n+1} m_0]} \right. \\
&\quad \left. + \frac{[\partial_\tau \theta_n - (\partial_\tau x_n)(-1)^{n+1} m_0]^2}{[\partial_\tau \theta_n - (\partial_\tau x_n)(-1)^{n+1} m_0]} \right\} \\
&= \frac{1}{3} \sum_n \left[(x_{2n+1} - x_{2n}) (\dot{a}_{2n+1}^2 + \dot{a}_{2n+1} \dot{a}_{2n} + \dot{a}_{2n}^2) + (x_{2n} - x_{2n-1}) (\dot{b}_{2n}^2 + \dot{b}_{2n} \dot{b}_{2n-1} + \dot{b}_{2n-1}^2) \right]. \quad (C13)
\end{aligned}$$

3. Dissipative action

As we discuss in main text, an important momentum relaxation mechanism is through the scattering between domain walls and phonons give rise to a phonon drag. Here, we describe the dissipative action in the Lagrangian coordinate. With the standard treatment [81, 82], the dissipative action (corresponding to phonon drag force $F = -\gamma v$) is given by

$$\mathcal{S}_{\text{dis}} = \frac{\gamma}{2} \frac{1}{\beta} \sum_{\omega_m} \sum_n |\omega_m| x_n(-\omega_m) x_n(\omega_m) = \frac{\gamma}{4m_0\beta} \sum_{\omega_m} \sum_n |\omega_m| [a_n(-\omega_m) - b_n(-\omega_m)] [a_n(\omega_m) - b_n(\omega_m)]. \quad (C14)$$

This dissipative action is crucial in the linear-response calculations as it generates an Ohmic response.

4. Vector potential and response

In this section, we discuss the derivation of linear-response in the presence of a small vector potential A . Our goal is to derive an effective action of A by integrating out all the fluctuating domain-wall degrees of freedom at the Gaussian level. The quadratic coefficient of A^2 term in the effective action corresponds to the linear-response coefficient.

In the presence of a vector potential, we can perform the minimal substitution: $\partial_x \theta \rightarrow \partial_x \theta - A$. The V term becomes

$$V = \sum_n \int_n^{n+1} ds (x_{n+1} - x_n) \left\{ \frac{|r|}{4m_0^2} [(\partial_x \theta - A)^2 - m_0^2]^2 + \frac{1}{2} (\partial_x^2 \theta - \partial_x A)^2 \right\} \quad (C15)$$

$$= \sum_n \int_n^{n+1} ds (x_{n+1} - x_n) \left\{ \begin{aligned} &\frac{|r|}{4m_0^2} [(\partial_x \theta)^2 - m_0^2]^2 + \frac{1}{2} (\partial_x^2 \theta)^2 \\ &- A \frac{|r|}{m_0^2} (\partial_x \theta) [(\partial_x \theta)^2 - m_0^2] - (\partial_x A) (\partial_x^2 \theta) \\ &+ A^2 \frac{|r|}{2m_0^2} [3(\partial_x \theta)^2 - m_0^2] + \frac{1}{2} (\partial_x A)^2 \end{aligned} \right\} + O(A^3), \quad (C16)$$

where we keep upto A^2 order in the spirit of linear response. To incorporate the response to the vector potential, we assume that $\partial_x \theta = (-1)^{n+1} m_0 + h(x)$ for $x_n < x < x_{n+1}$, where $h(x)$ is a response due to A and is given by

$$h(x) = \partial_x \theta - (-1)^{n+1} m_0 = \frac{\theta_{n+1} - \theta_n - (-1)^{n+1} m_0 (x_{n+1} - x_n)}{x_{n+1} - x_n} = \frac{\sqrt{2}}{x_{n+1} - x_n} \times \begin{cases} (a_{n+1} - a_n), & \text{for } n \text{ is even,} \\ (b_{n+1} - b_n), & \text{for } n \text{ is odd.} \end{cases} \quad (C17)$$

Thus, we expand V upto $O(h^2)$ as follows:

$$V \approx \sum_n \int_n^{n+1} ds (x_{n+1} - x_n) \left\{ \begin{aligned} &\frac{|r|}{4m_0^2} [2(-1)^{n+1} m_0 h + h^2]^2 + \frac{1}{2} (\partial_x h)^2 \\ &- A \frac{|r|}{m_0^2} ((-1)^{n+1} m_0 + h) [2(-1)^{n+1} m_0 h + h^2] - (\partial_x A) (\partial_x h) \\ &+ A^2 \frac{|r|}{2m_0^2} [2m_0^2 + 6(-1)^{n+1} m_0 h + 3h^2] + \frac{1}{2} (\partial_x A)^2 \end{aligned} \right\} \quad (C18)$$

$$= \sum_n \int_n^{n+1} ds (x_{n+1} - x_n) \left\{ \begin{aligned} &|r| h^2 + \frac{1}{2} (\partial_x h)^2 \\ &- A \frac{|r|}{m_0^2} (2m_0^2 h) - (\partial_x A) (\partial_x h) \\ &+ A^2 \frac{|r|}{2m_0^2} [2m_0^2] + \frac{1}{2} (\partial_x A)^2 \end{aligned} \right\} + O(h^3, Ah^2, A^2 h) \quad (C19)$$

We further ignore the terms involving $\partial_x h$ as they are not important for our purpose. The potential term becomes

$$\begin{aligned}
V \approx & \int dx \left[|r|A^2 + \frac{1}{2}(\partial_x A)^2 \right] \\
& + \sum_n \int_{2n}^{2n+1} ds(x_{2n+1} - x_{2n}) \left\{ \frac{2|r|}{(x_{2n+1} - x_{2n})^2} (a_{2n+1} - a_{2n})^2 - \frac{2\sqrt{2}|r|A(a_{2n+1} - a_{2n})}{(x_{2n+1} - x_{2n})} \right\} \\
& + \sum_n \int_{2n-1}^{2n} ds(x_{2n} - x_{2n-1}) \left\{ \frac{2|r|}{(x_{2n} - x_{2n-1})^2} (b_{2n} - b_{2n-1})^2 - \frac{2\sqrt{2}|r|A(b_{2n} - b_{2n-1})}{(x_{2n} - x_{2n-1})} \right\} \quad (C20)
\end{aligned}$$

Using Eq. (C17), the kinetic energy is expressed by:

$$\begin{aligned}
K &= \frac{1}{6} \sum_n (x_{n+1} - x_n) \left\{ \begin{aligned} & [\partial_\tau \theta_{n+1} - (\partial_\tau x_{n+1})(-1)^{n+1}m_0 - (\partial_\tau x_{n+1})h]^2 \\ & + [\partial_\tau \theta_{n+1} - (\partial_\tau x_{n+1})(-1)^{n+1}m_0 - (\partial_\tau x_{n+1})h] [\partial_\tau \theta_n - (\partial_\tau x_n)(-1)^{n+1}m_0 - (\partial_\tau x_n)h] \\ & + [\partial_\tau \theta_n - (\partial_\tau x_n)(-1)^{n+1}m_0 - (\partial_\tau x_n)h]^2 \end{aligned} \right\} \\
&= \frac{1}{3} \sum_n \left[(x_{2n+1} - x_{2n}) (\dot{a}_{2n+1}^2 + \dot{a}_{2n}^2 + \dot{a}_{2n+1}\dot{a}_{2n}) + (x_{2n} - x_{2n-1}) (\dot{b}_{2n-1}^2 + \dot{b}_{2n}^2 + \dot{b}_{2n-1}\dot{b}_{2n}) \right] + O(a^3, b^3, a^2b, ab^2),
\end{aligned}$$

where the higher order terms are ignored.

Our goal is to derive an effective action $\mathcal{S}_{A,\text{eff}}[A]$ by integrating out a_n and b_n at the Gaussian level. Formally, we consider

$$\begin{aligned}
& \hat{\Phi}^\dagger \hat{M} \hat{\Phi} + \hat{\xi}^\dagger \hat{\Phi} + \hat{\Phi}^\dagger \hat{\xi} \\
& = \left(\hat{\Phi}^\dagger + \hat{\xi}^\dagger \hat{M}^{-1} \right) \hat{M} \left(\hat{\Phi} + \hat{M}^{-1} \hat{\xi} \right) - \hat{\xi}^\dagger \hat{M}^{-1} \hat{\xi}, \quad (C21)
\end{aligned}$$

where $\hat{\Phi}$ is a $2N$ -dimensional vector made of a_n and b_n (with N being the number of domain walls), $\hat{\xi}$ is a $2N$ -dimensional vector, and \hat{M} is a $(2N) \times (2N)$ matrix. $\hat{\xi}$

and \hat{M} are functions of A . Particularly, $\hat{\xi}$ vanishes when $A \rightarrow 0$. Since we are interested in the correction to A^2 order, we drop $O(A^2)$ in $\hat{\xi}$. Similarly, we keep only the $O(A^0)$ terms in \hat{M} . Moreover, we drop $\partial_x a_n$ and $\partial_x b_n$ terms because they don't contribute to ac conductivity or stiffness in the limit we are interested in.

In addition, we ignore the fluctuation of the domain size and assume that $x_{n+1} - x_n = \bar{l}$. Such an assumption is valid when the domain size is sufficiently large and the Casimir potential coefficient $\mathcal{C} \gg 1$. The action associated with K is as follows:

$$\mathcal{S}_K \approx \frac{\bar{l}}{3} \int d\tau \sum_n \left[\dot{a}_{2n+1}^2 + \dot{a}_{2n}^2 + \dot{a}_{2n+1}\dot{a}_{2n} + \dot{b}_{2n-1}^2 + \dot{b}_{2n}^2 + \dot{b}_{2n-1}\dot{b}_{2n} \right] \quad (C22)$$

$$= \frac{\bar{l}}{3} \frac{1}{\beta} \sum_{\omega_m} \sum_k \omega_m^2 \left[\begin{aligned} & \tilde{a}_1(-\omega_m, -k) \tilde{a}_1(\omega_m, k) + \tilde{a}_0(-\omega_m, -k) \tilde{a}_0(\omega_m, k) \\ & + \frac{1}{2} \tilde{a}_1(-\omega_m, -k) \tilde{a}_0(\omega_m, k) + \frac{1}{2} \tilde{a}_0(-\omega_m, -k) \tilde{a}_1(\omega_m, k) \\ & + \tilde{b}_1(-\omega_m, -k) \tilde{b}_1(\omega_m, k) + \tilde{b}_0(-\omega_m, -k) \tilde{b}_0(\omega_m, k) \\ & + \frac{e^{i2k\bar{l}}}{2} \tilde{b}_1(-\omega_m, -k) \tilde{b}_0(\omega_m, k) + \frac{e^{-i2k\bar{l}}}{2} \tilde{b}_0(-\omega_m, -k) \tilde{b}_1(\omega_m, k) \end{aligned} \right]. \quad (C23)$$

In the above expressions, we have assumed periodic boundary condition and introduced the Fourier modes as follows:

$$\tilde{a}_0(k) = \frac{1}{\sqrt{N/2}} \sum_n e^{-i2k\bar{l}n} a_{2n}, \quad \tilde{a}_1(k) = \frac{1}{\sqrt{N/2}} \sum_n e^{-i2k\bar{l}n} a_{2n+1}, \quad (C24)$$

$$\tilde{b}_0(k) = \frac{1}{\sqrt{N/2}} \sum_n e^{-i2k\bar{l}n} b_{2n}, \quad \tilde{b}_1(k) = \frac{1}{\sqrt{N/2}} \sum_n e^{-i2k\bar{l}n} b_{2n+1}, \quad (C25)$$

where N is the number of domains. The unit cell size is $2\bar{l}$ and contains 2 a 's and 2 b 's.

The action associated with V is given by $\mathcal{S}'_V + \mathcal{S}_{A,0}$

$$\begin{aligned} \mathcal{S}'_V \approx & \int d\tau \sum_n \left\{ \begin{aligned} & \frac{2|r|}{l} (a_{2n+1} - a_{2n})^2 - 2\sqrt{2}|r|A (a_{2n+1} - a_{2n}) \\ & + \frac{2|r|}{l} (b_{2n} - b_{2n-1})^2 - 2\sqrt{2}|r|A (b_{2n} - b_{2n-1}) \end{aligned} \right\} \\ & = \frac{1}{\beta} \sum_{\omega_m, k} \left\{ \begin{aligned} & \frac{2|r|}{l} [\tilde{a}_0(-\omega_m, -k)\tilde{a}_0(\omega_m, k) + \tilde{a}_1(-\omega_m, -k)\tilde{a}_1(\omega_m, k) - \tilde{a}_0(-\omega_m, -k)\tilde{a}_1(\omega_m, k) - \tilde{a}_1(-\omega_m, -k)\tilde{a}_0(\omega_m, k)] \\ & - \sqrt{2}|r|A(-\omega_n, -k) [\tilde{a}_1(\omega_n, k) - \tilde{a}_0(\omega_n, k)] - \sqrt{2}|r| [\tilde{a}_1(-\omega_n, -k) - \tilde{a}_0(-\omega_n, -k)] A(\omega_n, k) \\ & + \frac{2|r|}{l} [\tilde{b}_0(-\omega_m, -k)\tilde{b}_0(\omega_m, k) + \tilde{b}_1(-\omega_m, -k)\tilde{b}_1(\omega_m, k) - e^{-i2k\bar{l}}\tilde{b}_0(-\omega_m, -k)\tilde{b}_1(\omega_m, k) - e^{i2k\bar{l}}\tilde{b}_1(-\omega_m, -k)\tilde{b}_0(\omega_m, k)] \\ & - \sqrt{2}|r|A(-\omega_n, -k) [e^{-i2k\bar{l}}\tilde{b}_1(\omega_n, k) - \tilde{b}_0(\omega_n, k)] - \sqrt{2}|r| [e^{i2k\bar{l}}\tilde{b}_1(-\omega_n, -k) - \tilde{b}_0(-\omega_n, -k)] A(\omega_n, k) \end{aligned} \right\}, \end{aligned} \quad (\text{C26})$$

(C27)

$$\mathcal{S}_{A,0} = \int d\tau dx \left[|r|A^2 + \frac{1}{2}(\partial_x A)^2 \right]. \quad (\text{C28})$$

Our goal is to derive the correction to the $|r|A^2$ term in $\mathcal{S}_{A,0}$.

With the expressions of various actions, we are in the position to integrate out the a_n and b_n variables. The $\mathcal{S}_K + \mathcal{S}'_V + \mathcal{S}_{\text{dis}}$ can be expressed by

$$\mathcal{S}_K + \mathcal{S}'_V + \mathcal{S}_{\text{dis}} = \frac{1}{2\beta} \sum_{\omega_m, k} \left[\hat{\Phi}_{\omega_m, k}^\dagger \hat{M}(\omega_m, k) \hat{\Phi}_{-\omega_m, -k} + \hat{\xi}_{\omega_m, k}^\dagger \hat{\Phi}_{\omega_m, k} + \hat{\Phi}_{\omega_m, k}^\dagger \hat{\xi}_{\omega_m, k} \right], \quad (\text{C29})$$

where

$$\hat{M}(\omega_m, k) = \frac{2\bar{l}}{3}\omega_m^2 \begin{bmatrix} 1 & 0 & 1/2 & 0 \\ 0 & 1 & 0 & e^{-i2k\bar{l}}/2 \\ 1/2 & 0 & 1 & 0 \\ 0 & e^{i2k\bar{l}}/2 & 0 & 1 \end{bmatrix} + \frac{4|r|}{\bar{l}} \begin{bmatrix} 1 & 0 & -1 & 0 \\ 0 & 1 & 0 & -e^{-i2k\bar{l}} \\ -1 & 0 & 1 & 0 \\ 0 & -e^{i2k\bar{l}} & 0 & 1 \end{bmatrix} + \frac{\gamma}{2m_0}|\omega_m| \begin{bmatrix} 1 & -1 & 0 & 0 \\ -1 & 1 & 0 & 0 \\ 0 & 0 & 1 & -1 \\ 0 & 0 & -1 & 1 \end{bmatrix}, \quad (\text{C30})$$

$$\hat{\xi}_{\omega_m, k} = A(\omega_m, k) \begin{bmatrix} 2\sqrt{2}|r| \\ 2\sqrt{2}|r| \\ -2\sqrt{2}|r| \\ -2\sqrt{2}|r|e^{-i2k\bar{l}} \end{bmatrix}, \quad (\text{C31})$$

$$\hat{\Phi}_{\omega_m, k} = \begin{bmatrix} a_0(\omega_m, k) \\ b_0(\omega_m, k) \\ a_1(\omega_m, k) \\ b_1(\omega_m, k) \end{bmatrix}. \quad (\text{C32})$$

The effective action for \tilde{A} is given by

$$\begin{aligned} \mathcal{S}_{A,\text{eff}} &= \mathcal{S}_{A,0} - \frac{1}{2\beta} \sum_{\omega_m, k} \hat{\xi}_{\omega_m, k}^\dagger \hat{M}^{-1}(\omega_m, k) \hat{\xi}_{\omega_m, k} \\ &= \frac{2\bar{l}|r|}{\beta} \sum_{\omega_m, k} A(-\omega_m, -k) A(\omega_m, k) \\ &\quad - \frac{1}{2\beta} \sum_{\omega_m, k} \hat{\xi}_{\omega_m, k}^\dagger \hat{M}^{-1}(\omega_m, k) \hat{\xi}_{\omega_m, k}. \end{aligned} \quad (\text{C33})$$

Note that the unit cell size is $2\bar{l}$. Using Mathematica and taking the long-wavelength limits, we obtain two asymptotic results

$$\begin{aligned} &\frac{1}{2} \hat{\xi}_{\omega_m, k}^\dagger \hat{M}^{-1}(\omega_m, k) \hat{\xi}_{\omega_m, k} \Big|_{k=0, \omega_m \rightarrow 0} \\ &\rightarrow \frac{16m_0|r|^2\gamma\bar{l}A(-\omega_m, 0)A(\omega_m, 0)}{8m_0|r|\gamma + (8m_0^2|r| + \gamma^2)|\omega_m|\bar{l}}, \end{aligned} \quad (\text{C34})$$

$$\begin{aligned} &\frac{1}{2} \hat{\xi}_{\omega_m, k}^\dagger \hat{M}^{-1}(\omega_m, k) \hat{\xi}_{\omega_m, k} \Big|_{k=0, \gamma=0} \\ &\rightarrow \frac{48|r|\bar{l}^2}{24|r| + \omega_m^2\bar{l}^2} A(-\omega_m, 0)A(\omega_m, 0), \end{aligned} \quad (\text{C35})$$

Thus, the effective action for \tilde{A} (with $k=0$) is given by

$$\begin{aligned} \mathcal{S}_{A,\text{eff}} \Big|_{k=0} &\equiv \frac{\bar{l}}{\beta} \sum_{\omega_m} Q(\omega_m) \tilde{A}(-\omega_m) \tilde{A}(\omega_m) \\ &= \frac{2\bar{l}}{\beta} \sum_{\omega_m} |r| \tilde{A}(-\omega_m) \tilde{A}(\omega_m) - \frac{1}{2} \hat{\xi}_{\omega_m, k}^\dagger \hat{M}^{-1}(\omega_m, k) \hat{\xi}_{\omega_m, k} \Big|_{k=0}. \end{aligned} \quad (\text{C36})$$

With a nonzero γ , the low-frequency ac conductivity (σ_{ac}) and stiffness (ρ_s) are given by

$$\begin{aligned} \sigma_{\text{ac}}(i\omega_m) &\propto \frac{1}{\omega_m} Q(\omega_m) \\ \rightarrow \sigma_{\text{ac}}(\omega) &\propto \frac{i}{\omega} \left[2|r| - \frac{16m_0|r|^2\gamma}{8m_0|r|\gamma + (8m_0^2|r| + \gamma^2)(-i\omega)\bar{l}} \right], \end{aligned} \quad (\text{C37})$$

$$\rightarrow \text{Re}[\sigma_{\text{ac}}(\omega)] \propto \frac{16m_0|r|^2\gamma(8m_0^2|r| + \gamma^2)\bar{l}}{(8m_0|r|\gamma)^2 + [(8m_0^2|r| + \gamma^2)\omega\bar{l}]^2}, \quad (\text{C38})$$

$$\rho_s \propto Q(\omega_m=0) = 0. \quad (\text{C39})$$

We note that we have performed analytic continuation from Matsubara frequencies to real frequencies. See [81, 82] for discussion on the analytic continuation of the phonon drag contribution in the response function. Equation (C38) is consistent with the Drude formula in the low-frequency limit, i.e. the real part of ac conductivity is nonzero for $\omega \rightarrow 0$.

In the absence of phonon drag (i.e., $\gamma=0$), a_n and b_n are decoupled in Eq. (C29). As a result, \hat{M} can be block

diagonalized. We can easily perform a similar analysis and show that

$$\sigma_{\text{ac}}(\omega)|_{\gamma=0} \propto \frac{i}{\omega} \left(2|r| - \frac{2|r|^2}{|r| - \omega^2\bar{l}^2/24} \right), \quad (\text{C40})$$

$$\rho_s|_{\gamma=0} = 0, \quad (\text{C41})$$

resulting in zero superfluid stiffness and the absence of Ohmic response.

Appendix D: Hydrodynamics near quantum Lifshitz critical point

The effective action S_{eff} in the real-time path integral is given by

$$\begin{aligned} \mathcal{S} &= \int dt dx \mathcal{L} \\ &= \int dt dx \left[\frac{1}{2} (\partial_t \theta)^2 - \frac{1}{2} (\partial_x^2 \theta)^2 - \frac{r}{2} (\partial_x \theta)^2 - u (\partial_x \theta)^4 \right], \end{aligned} \quad (\text{D1})$$

where \mathcal{L} is the Lagrangian density, and θ is a real-valued bosonic field. The equation of motion can be derived by the Euler-Lagrange equation (with higher order derivative terms) and is given by

$$\begin{aligned} \delta \mathcal{S} &= 0 \\ \rightarrow \frac{\partial \mathcal{L}}{\partial \theta} - \frac{\partial}{\partial t} \left[\frac{\partial \mathcal{L}}{\partial (\partial_t \theta)} \right] - \frac{\partial}{\partial x} \left[\frac{\partial \mathcal{L}}{\partial (\partial_x \theta)} \right] + \frac{\partial^2}{\partial x^2} \left[\frac{\partial \mathcal{L}}{\partial (\partial_x^2 \theta)} \right] &= 0 \end{aligned} \quad (\text{D2})$$

$$\begin{aligned} \rightarrow -(\partial_t^2 \theta) + r(\partial_x^2 \theta) + 4u \partial_x \left[(\partial_x \theta)^3 \right] - (\partial_x^4 \theta) &= 0 \\ \rightarrow \partial_t (\partial_t \theta) - \partial_x \left[r(\partial_x \theta) + 4u(\partial_x \theta)^3 - \partial_x^3 \theta \right] &= 0. \end{aligned} \quad (\text{D3})$$

The momentum density conjugate to $\theta(x)$ is given by

$$\Pi(x) \equiv \frac{\partial \mathcal{L}}{\partial (\partial_t \theta)} = \partial_t \theta. \quad (\text{D4})$$

The Hamiltonian density is given by

$$\mathcal{H} = \Pi(\partial_t \theta) - \mathcal{L} = \frac{1}{2} \Pi^2 + \frac{1}{2} (\partial_x^2 \theta)^2 + \frac{r}{2} (\partial_x \theta)^2 + u (\partial_x \theta)^4. \quad (\text{D5})$$

1. Current and stress tensor

The physical density and current operators are given by

$$j_t(x, t) = -\partial_t \theta - A_0, \quad (\text{D6})$$

$$j_x(x, t) = r(\partial_x \theta) + 4u(\partial_x \theta)^3 - \partial_x^3 \theta, \quad (\text{D7})$$

where $A_0 \neq 0$ corresponds to a finite density of bosons. Note that we define j_t with a minus sign. The continuity equation $\partial_t j_t + \partial_x j_x = 0$ is ensured by the Euler-Lagrangian equation. Since the θ -only action is derived

in the high density limit, we consider a Lagrangian density with a finite A_0 given by

$$\mathcal{L} = \frac{1}{2} (\partial_t \theta)^2 - \frac{1}{2} (\partial_x^2 \theta)^2 - \frac{r}{2} (\partial_x \theta)^2 - u (\partial_x \theta)^4 + A_0 (\partial_t \theta). \quad (\text{D8})$$

The finite-temperature scaling of sound velocity depends on whether A_0 is nonzero.

To derive the energy-momentum stress tensor, we focus on translation operations. We consider $x^\mu \rightarrow x^\mu - a^\mu$. Alternatively, the field is transformed by

$$\theta(x) \rightarrow \theta(x + a) = \theta(x) + a^\mu \partial_\mu \theta(x). \quad (\text{D9})$$

In this case, the Lagrangian density is transformed in the following way, $\mathcal{L} \rightarrow \mathcal{L} + a^\nu \partial_\nu (\delta^\mu \mathcal{L})$. We find that

$$\begin{aligned} & a^0 \left\{ \partial_t \left[\frac{\partial \mathcal{L}}{\partial (\partial_t \theta)} (\partial_t \theta) - \mathcal{L} \right] + \partial_x \left[\frac{\partial \mathcal{L}}{\partial (\partial_x \theta)} (\partial_x \theta) + \frac{\partial \mathcal{L}}{\partial (\partial_x^2 \theta)} (\partial_x \partial_t \theta) - \partial_x \left(\frac{\partial \mathcal{L}}{\partial (\partial_x^2 \theta)} \right) (\partial_t \theta) \right] \right\} \\ & + a^1 \left\{ \partial_t \left[\frac{\partial \mathcal{L}}{\partial (\partial_t \theta)} (\partial_x \theta) \right] + \partial_x \left[\frac{\partial \mathcal{L}}{\partial (\partial_x \theta)} (\partial_x \theta) + \frac{\partial \mathcal{L}}{\partial (\partial_x^2 \theta)} (\partial_x^2 \theta) - \partial_x \left(\frac{\partial \mathcal{L}}{\partial (\partial_x^2 \theta)} \right) (\partial_x \theta) - \mathcal{L} \right] \right\} = 0 \end{aligned} \quad (\text{D10})$$

The stress tensor is defined by

$$T_{tt} = \frac{\partial \mathcal{L}}{\partial (\partial_t \theta)} (\partial_t \theta) - \mathcal{L} = \frac{1}{2} (\partial_t \theta)^2 + \frac{1}{2} (\partial_x^2 \theta)^2 + \frac{r}{2} (\partial_x \theta)^2 + u (\partial_x \theta)^4 = \mathcal{H}, \quad (\text{D11})$$

$$T_{xt} = \frac{\partial \mathcal{L}}{\partial (\partial_t \theta)} (\partial_x \theta) = (\partial_t \theta) (\partial_x \theta) + A_0 (\partial_x \theta), \quad (\text{D12})$$

$$T_{tx} = \frac{\partial \mathcal{L}}{\partial (\partial_x \theta)} (\partial_t \theta) + \frac{\partial \mathcal{L}}{\partial (\partial_x^2 \theta)} (\partial_x \partial_t \theta) - \partial_x \left(\frac{\partial \mathcal{L}}{\partial (\partial_x^2 \theta)} \right) (\partial_t \theta) \quad (\text{D13})$$

$$= \left[-r (\partial_x \theta) - 4u (\partial_x \theta)^3 + (\partial_x^3 \theta) \right] (\partial_t \theta) - (\partial_x^2 \theta) (\partial_x \partial_t \theta), \quad (\text{D14})$$

$$T_{xx} = \frac{\partial \mathcal{L}}{\partial (\partial_x \theta)} (\partial_x \theta) + \frac{\partial \mathcal{L}}{\partial (\partial_x^2 \theta)} (\partial_x^2 \theta) - \partial_x \left(\frac{\partial \mathcal{L}}{\partial (\partial_x^2 \theta)} \right) (\partial_x \theta) - \mathcal{L} \quad (\text{D15})$$

$$= -\frac{1}{2} (\partial_t \theta)^2 - \frac{1}{2} (\partial_x^2 \theta)^2 - \frac{r}{2} (\partial_x \theta)^2 - 3u (\partial_x \theta)^4 + (\partial_x^3 \theta) (\partial_x \theta) - A_0 (\partial_t \theta), \quad (\text{D16})$$

We can easily check that $\partial_t T_{tt} + \partial_x T_{tx} = 0$ and $\partial_t T_{xt} + \partial_x T_{xx} = 0$.

2. Gaussian fixed point

Now, we determine the scaling dimensions of operators and RG eigenvalues of coupling constants in the action given by Eq. (D1). First, we focus on the scaling near the Gaussian fixed point, corresponding to

$$[x] = -1, [t] = -z, [\theta] = -\frac{\epsilon}{2}, y_r = 2, y_u = \epsilon, \quad (\text{D17})$$

where $\epsilon = 2 - d = 1$ in our case. Notice that $[\theta]$ does not explicitly depend on y_r or y_u . Then, we examine the scaling dimensions of $T_{\mu\nu}$ and j_μ in the following.

In our theory with a finite density, A_0 is a constant that does not scale under RG. Thus, $[A_0] = 0$. We focus on the leading scaling dimension of $[T_{xt}]$ and $[T_{xx}]$, which are given by $[\partial_x \theta]$ and $[\partial_t \theta]$ respectively. Based on dimensional analysis, we derive

$$\begin{aligned} y_\beta &= -2, [T_{tt}] = 3, [T_{xt}] = \frac{1}{2}, [T_{tx}] = 4, \\ [T_{xx}] &= \frac{3}{2}, [j_t] = 0, [j_x] = \frac{5}{2}. \end{aligned} \quad (\text{D18})$$

Note that $[T_{tt}] = z + d$ holds for quantum Lifshitz field theory [83, 84]. Here, $z = 2$ and $d = 1$.

3. Interacting fixed point

We are interested in the results near the interacting fixed point. We first recall the RG equations [63] at order $O(\epsilon)$ given by

$$\frac{dr}{dl} = 2r + \frac{3u}{\pi} \left(\Lambda^2 - \frac{1}{2} r \right), \quad (\text{D19})$$

$$\frac{du}{dl} = \epsilon u - \frac{9}{2\pi} u^2. \quad (\text{D20})$$

The fixed point is given by $(r^*, u^*) = (-\epsilon \Lambda^2 / 3, 2\pi / 9)$ (upto linear-in- ϵ order). The RG dimensions for r and $w = \frac{9\Lambda^2}{4\pi(\epsilon-3)} r + u$ are $y_r = 2 - \epsilon/3$ and $y_w = \epsilon - 2$. Since u is no longer the eigen direction of the RG flow,

the scaling of u has two contributions. At the end of the calculations, we will set $\epsilon = 1$.

Now we discuss the scaling dimensions of $T_{\mu\nu}$ and j_μ near the interacting fixed point. We can easily show that j_t , $[T_{tt}]$, $[T_{xt}]$ are unchanged. Then, we use conservation laws and obtain the same scaling results for j_x , $[T_{tx}]$, $[T_{xx}]$. Therefore, the scaling dimensions of $T_{\mu\nu}$ and j_μ remain the same as that in the Gaussian fixed point.

4. Free energy in quantum critical regime

To construct a hydrodynamic theory, we consider a free energy $F[\mu, \beta, v]$ defined by

$$e^{-\beta F[s, \mu, \beta, v]} = e^{-L f[s, \mu, \beta, v]} = \text{Tr} \left[e^{-\beta \int dx (s T_{tt} - v T_{xt} - \mu j_t)} \right], \quad (\text{D21})$$

where β is the inverse temperature, s is a dimensionless parameter (s is set to 1 at the end of calculations), v is the center of mass velocity, μ is the chemical potential, L is the system size, and f is the reduced free energy density. In this formulation, $H = \int dx T_{tt}$ (energy), $P = \int dx T_{xt}$ (momentum), and $N = \int dx j_t$ (particle number) are the conserved quantity of the theory. Our goal here is to extract the scaling behavior of various hydrodynamic quantities in the quantum critical scaling region defined by $\xi_T < \xi$ (ξ_T is the thermal wavelength and ξ is the correlation length of the theory).

In the quantum critical regime, the temperature dependence can be determined by the hyper-scaling. The reduced free energy density near the critical point obeys the following scaling relation

$$f[s, \mu, \beta, v] = b^{-d} f[s, \mu b^{y_\mu}, \beta b^{-z}, v b^{y_v}], \quad (\text{D22})$$

where b is the scale parameter, $z = 2$ is the dynamic exponent, y_v is the scaling eigenvalue of v , and y_μ is the scaling eigenvalue of μ . We can fix βb^{-z} to a constant and rewrite the expression in terms of $T = 1/\beta$ as follows

$$f[s, \mu, \beta, v] = T^{\frac{d}{z}} \Phi \left[s, \frac{\mu}{T^{\frac{y_\mu}{z}}}, \frac{v}{T^{\frac{y_v}{z}}} \right], \quad (\text{D23})$$

where Φ is a universal scaling function. Recall that $\beta F = Lf$, we obtain the free energy density

$$F[s, \mu, 1/T, v]/L = T^{1+\frac{d}{z}} \Phi \left[s, \frac{\mu}{T^{\frac{y_\mu}{z}}}, \frac{v}{T^{\frac{y_v}{z}}} \right]. \quad (\text{D24})$$

With the expression of the free energy density, we can derive the following expectation values:

$$\langle T_{tt} \rangle = \frac{1}{L} \left(\frac{\partial F}{\partial s} \right)_{v, \mu, T} \Big|_{s=1} \sim T^{1+\frac{d}{z}} = T^{3/2} \quad (\text{D25})$$

$$\langle T_{xt} \rangle = -\frac{1}{L} \left(\frac{\partial F}{\partial v} \right)_{T, \mu, s} \Big|_{s=1} \sim T^{1+\frac{d-y_v}{z}} = T^{1/4}, \quad (\text{D26})$$

$$\langle j_t \rangle = -\frac{1}{L} \left(\frac{\partial F}{\partial \mu} \right)_{T, v, s} \Big|_{s=1} \sim T^{1+\frac{d-y_\mu}{z}} = T^0, \quad (\text{D27})$$

where we have used $y_v = 5/2$ and $y_\mu = 3$. We also assumed the translation symmetry and analyticity in the scaling function. Using the scaling results in Eq. (D18), we derive that

$$\langle T_{tx} \rangle \sim T^2, \quad \langle T_{xx} \rangle \sim T^{3/4}, \quad \langle j_x \rangle \sim T^{1/4}. \quad (\text{D28})$$

To derive $[j_x]$, we use $[\delta j_t] \sim T^{3/4}$ as the A_0 term does not contribute.

Now, we are in the position to determine the scaling of various thermodynamic quantities. These thermodynamic quantities are given by

$$\delta \langle T_{tt} \rangle / \delta \beta = C_\beta \sim T^{5/2}, \quad (\text{D29})$$

$$\delta \langle T_{tt} \rangle / \delta \mu = C_\mu \sim T^0, \quad (\text{D30})$$

$$\delta \langle T_{xx} \rangle / \delta \beta = K_\beta \sim T^{7/4}, \quad (\text{D31})$$

$$\delta \langle T_{xx} \rangle / \delta \mu = K_\mu \sim T^{-3/4}, \quad (\text{D32})$$

$$\delta \langle j_t \rangle / \delta \beta = \chi_\beta \sim T^{7/4}, \quad (\text{D33})$$

$$\delta \langle j_t \rangle / \delta \mu = \chi_\mu \sim T^{-3/4}, \quad (\text{D34})$$

$$\delta \langle T_{xt} \rangle / \delta v = \rho_M \sim T^{-1}, \quad (\text{D35})$$

$$\delta \langle T_{tx} \rangle / \delta v = \rho_E \sim T^{3/4}, \quad (\text{D36})$$

$$\delta \langle j_x \rangle / \delta v = \rho_Q \sim T^0, \quad (\text{D37})$$

where we have used $[\delta j_t] \sim T^{3/4}$ as the A_0 term does not contribute. Again, we have used the scaling function Φ and the conservation laws for energy, momentum, and charge.

Note that $C_\beta \neq C_T = \delta \langle T_{tt} \rangle / \delta T \sim T^{1/2}$ ($C_T \sim T^{1/2}$ is consistent with Ref. [63]). $\rho_M \sim 1/T$ is also consistent with the magnetic susceptibility in Ref. [63]. For interacting bosons, ρ_M is the inertia, which is inversely proportional to the superfluid stiffness. Thus, we obtain that $\rho_s \sim \rho_M^{-1} \sim T$, which vanishes at zero temperature.

5. Sound velocity

The conservation laws for energy, momentum, and charge are given by

$$\partial_t \langle T_{tt} \rangle + \partial_x \langle T_{tx} \rangle = 0, \quad (\text{D38})$$

$$\partial_t \langle T_{xt} \rangle + \partial_x \langle T_{xx} \rangle = 0, \quad (\text{D39})$$

$$\partial_t \langle j_t \rangle + \partial_x \langle j_x \rangle = 0. \quad (\text{D40})$$

Using the thermodynamic relations, we obtain

$$\delta \langle T_{tt} \rangle = C_\beta \delta \beta + C_\mu \delta \mu, \quad (\text{D41a})$$

$$\delta \langle T_{tx} \rangle = \rho_E \delta v, \quad (\text{D41b})$$

$$\delta \langle T_{xt} \rangle = \rho_M \delta v, \quad (\text{D41c})$$

$$\delta \langle T_{xx} \rangle = K_\beta \delta \beta + K_\mu \delta \mu, \quad (\text{D41d})$$

$$\delta \langle j_t \rangle = \chi_\mu \delta \mu + \chi_\beta \delta \beta, \quad (\text{D41e})$$

$$\delta \langle j_x \rangle = \rho_Q \delta v. \quad (\text{D41f})$$

With Eq. (D41), the conservation laws can be recast as follows:

$$\begin{bmatrix} C_\mu & 0 & C_\beta \\ 0 & \rho_M & 0 \\ \chi_\mu & 0 & \chi_\beta \end{bmatrix} \partial_t \begin{bmatrix} \mu \\ v \\ \beta \end{bmatrix} + \begin{bmatrix} 0 & \rho_E & 0 \\ K_\mu & 0 & K_\beta \\ 0 & \rho_Q & 0 \end{bmatrix} \partial_x \begin{bmatrix} \mu \\ v \\ \beta \end{bmatrix} = 0 \quad (\text{D42})$$

Now, we use the property

$$\begin{aligned} \delta \begin{bmatrix} \langle T_{tt} \rangle \\ \langle T_{xt} \rangle \\ \langle j_t \rangle \end{bmatrix} &= \begin{bmatrix} C_\mu & 0 & C_\beta \\ 0 & \rho_M & 0 \\ \chi_\mu & 0 & \chi_\beta \end{bmatrix} \delta \begin{bmatrix} \mu \\ v \\ \beta \end{bmatrix} \\ \rightarrow \delta \begin{bmatrix} \mu \\ v \\ \beta \end{bmatrix} &= \begin{bmatrix} C_\mu & 0 & C_\beta \\ 0 & \rho_M & 0 \\ \chi_\mu & 0 & \chi_\beta \end{bmatrix}^{-1} \delta \begin{bmatrix} \langle T_{tt} \rangle \\ \langle T_{xt} \rangle \\ \langle j_t \rangle \end{bmatrix}. \end{aligned} \quad (\text{D43})$$

We find that the conservation law can be expressed by

$$\partial_t \begin{bmatrix} \epsilon \\ p \\ n \end{bmatrix} = \begin{bmatrix} 0 & M_4 & 0 \\ M_3 & 0 & M_2 \\ 0 & M_1 & 0 \end{bmatrix} \partial_x \begin{bmatrix} \epsilon \\ p \\ n \end{bmatrix}, \quad (\text{D44})$$

where $\epsilon = \langle T_{tt} \rangle$ is the energy density, $p = \langle T_{xt} \rangle$ is the momentum density, $n = \langle j_t \rangle$ is the number density, and $(M_1, M_2, M_3, M_4) = (\rho_Q/\rho_M, \frac{C_\mu K_\beta - C_\beta K_\mu}{C_\mu \chi_\beta - C_\beta \chi_\mu}, \frac{K_\mu \chi_\beta - K_\beta \chi_\mu}{C_\mu \chi_\beta - C_\beta \chi_\mu}, \rho_E/\rho_M)$. The eigenvalues of the matrix in Eq. (D44) correspond to the sound velocities. We find that $v = 0, \pm v_s$, where

$$v_s = \sqrt{M_1 M_2 + M_3 M_4}. \quad (\text{D45})$$

The corresponding normal modes are given by

$$\hat{n}_0 \propto \begin{bmatrix} -M_2 \\ 0 \\ M_3 \end{bmatrix}, \quad \hat{n}_\pm \propto \begin{bmatrix} M_4 \\ \pm v_s \\ M_1 \end{bmatrix}. \quad (\text{D46})$$

Based on the scaling analysis above, $M_1 \sim T$, $M_2 \sim T^0$, $M_3 \sim T^{-3/4}$, and $M_4 \sim T^{7/4}$. Thus, $M_1 M_2 \sim T$ and $M_3 M_4 \sim T$. Thus, the sound velocity $v_s \sim T^{1/2}$.

6. Classical gases with Lifshitz dispersion

It is also interesting to know the finite-temperature behavior in the classical gases with Lifshitz dispersion. To study this, we construct the partition function of N classical gases with Lifshitz dispersion as follows:

$$Z = \frac{1}{N!} \int \prod_{i=1}^N \left[\frac{dx_i dk_i}{2\pi} e^{-\beta(k_i^4 - vk_i)} \right] \quad (\text{D47})$$

$$= \frac{1}{N!} \left[L \beta^{-1/4} \Phi(v \beta^{3/4}) \right]^N, \quad (\text{D48})$$

where $\beta = 1/T$ is the inverse temperature and v is the velocity. We will set the v term to zero at the end of calculations.

The free energy is given by $F = -T \ln Z \approx -TN \ln \left[\frac{L\epsilon}{N} T^{1/4} \Phi(v/T^{3/4}) \right]$. The finite-temperature scaling of inertia can be obtained by $\frac{\partial^2 F}{\partial v^2} \sim T^{-1}$. Note that the result is qualitatively similar to the interacting quantum Lifshitz theory, but the exponent is different.

In addition, the sound velocity scaling can be derived. To do this, we obtain the expression of entropy through $S = -\frac{\partial F}{\partial T}$ and set $v = 0$. The entropy can be express as a function of $LT^{1/4}/N$. Then, we can easily derive the isentropic bulk modulus $K_s \sim T$, and the sound velocity $v_s \sim T^{1/2}$. Note that the sound velocity gives the same finite-temperature scaling as the interacting quantum Lifshitz theory despite the differences in detail.

The classical theory here is an approximate description for the interacting Lifshitz theory at sufficiently high temperature. Our results show that the inertia finite-temperature scaling is different in the high-temperature and in the quantum critical regime, while the sound velocity has the same finite-temperature scaling in both regimes.

Appendix E: Estimate of autocorrelation time

To understand the autocorrelation time in the interacting bosons with double-well dispersion, we first review several results in the transverse-field Ising model (TFIM) [68]. Then, we generalize the ideas for the momentum-momentum correlation function of interacting bosons with double-well dispersion.

The equal-time spin-spin correlation function of TFIM in the low-temperature symmetry-broken regime can be computed semicalssically. For a system $L \gg |x|$ with N thermally excited domain walls, the density is $\rho = N/L = 1/l_0$. The probability of finding a particle between 0 and x is given by $p = |x|/L$. It is crucial to note that each domain wall flips the sign of spin. With these ideas in mind, we can compute the expectation value of finding two equal-sign spins with a separation $|x|$ as follows:

$$C(x, 0) \propto \sum_{j=0}^N (-1)^j p^j (1-p)^{N-j} \frac{N!}{j!(N-j)!} \quad (\text{E1})$$

$$= (1-2p)^N = \left(1 - \frac{2|x|}{L} \right)^{L\rho} \rightarrow e^{-|x|/\xi_c}, \quad (\text{E2})$$

where $\xi_c = 1/(2\rho)$ dictates the length scale over which the spin correlation is missing. For TFIM, $\xi_c^{-1} = \sqrt{\frac{2\Delta T}{\pi c^2}} e^{-\Delta/T}$, c is the velocity of excitation (domain wall) in TFIM, and Δ is the energy cost of creating an excitation (domain wall)[67, 68] One can also compute the general space-time correlation function $C(x, t)$ using the same idea and averaging the ballistic propagation of domain walls [67, 68]. The idea is to estimate the time duration that a domain wall at $x = \xi_c$ travels to $x = 0$. In the end, one derive the equal-space autocorrelation function $C(0, t) \propto e^{-|t|/\tau_{\text{TFIM}}}$, where $\tau_{\text{TFIM}}^{-1} = \frac{2}{\pi} T e^{-\Delta/T}$ [67, 68].

A simple way to estimate autocorrelation time is to use $\bar{\tau}_{\text{TFIM}} = \xi_c/v_T$, where v_T is the thermal velocity obtained from the equipartition theorem. Since the dispersion of domain wall in TFIM is given by $\epsilon_k \approx \Delta + \frac{c^2 k^2}{2\Delta}$, we obtain $v_T = c\sqrt{T/\Delta}$. Then, we obtain $\bar{\tau}_{\text{TFIM}}^{-1} = \sqrt{\frac{2}{\pi}} T e^{-\Delta/T}$, which differs from τ_{TFIM}^{-1} by an overall numerical prefactor. Thus, this simple analysis seems to provide a reasonable estimate of the autocorrelation time.

Now, we discuss the interacting bosons with double-well dispersion. The momentum $\partial_x \theta$ here is analogous to the spin in TFIM. Using the same idea for TFIM, the equal-time correlation function $\langle \partial_x \theta(x, t) \partial_x \theta(0, t) \rangle \propto \exp(-|x|/\xi_c)$, where $\xi_c = l_0/2$. The autocorrelation function is significantly different because the constrained domain-wall motion and the phonon drag

induces a scattering time $\tau_{sc} = m/\gamma$, where $m \sim l_0$ is the mass of a moving domain. Since the scattering due to phonon drag is at random, we assume a random-walk process for the domain motion. Each scattering gives a move with a distance $\delta X \sim v'_T \tau_{sc}$, where $v'_T \sim \sqrt{T/l_0}$ is obtained from equipartition theorem. For M times of scattering, the total displacement due to random walk is given by $\delta X \sqrt{M}$. Using $M = \tau_{\text{DW}}/\tau_{sc}$ (with τ_{DW} being the autocorrelation time) and $\delta X \sqrt{M} = \xi_c$, we obtain $\tau_{\text{DW}} \sim \gamma l_0^2/T$ which is significantly larger than τ_{TFIM} in the low-temperature limit. For completeness, we discuss $\gamma = 0$ case. The analysis is similar to the autocorrelation time for TFIM except that the thermal velocity $v'_T \sim \sqrt{T/l_0}$. Therefore, we obtain $\tau'_{\text{DW}} \sim l_0^{3/2}/\sqrt{T}$, which is intermediate between τ_{TFIM} and τ_{DW} .

-
- [1] J. Stenger, S. Inouye, D. Stamper-Kurn, H.-J. Miesner, A. Chikkatur, and W. Ketterle, *Nature* **396**, 345 (1998).
- [2] M. Greiner, O. Mandel, T. Esslinger, T. W. Hänsch, and I. Bloch, *nature* **415**, 39 (2002).
- [3] T. Kinoshita, T. Wenger, and D. S. Weiss, *Science* **305**, 1125 (2004).
- [4] T. Kinoshita, T. Wenger, and D. S. Weiss, *Nature* **440**, 900 (2006).
- [5] L. Sadler, J. Higbie, S. Leslie, M. Vengalattore, and D. Stamper-Kurn, *Nature* **443**, 312 (2006).
- [6] Y.-J. Lin, K. Jiménez-García, and I. B. Spielman, *Nature* **471**, 83 (2011).
- [7] J.-Y. Zhang, S.-C. Ji, Z. Chen, L. Zhang, Z.-D. Du, B. Yan, G.-S. Pan, B. Zhao, Y.-J. Deng, H. Zhai, et al., *Phys. Rev. Lett.* **109**, 115301 (2012), URL <https://link.aps.org/doi/10.1103/PhysRevLett.109.115301>.
- [8] J. H. Nguyen, P. Dyke, D. Luo, B. A. Malomed, and R. G. Hulet, *Nature Physics* **10**, 918 (2014).
- [9] M. C. Beeler, R. A. Williams, K. Jimenez-Garcia, L. J. LeBlanc, A. R. Perry, and I. B. Spielman, *Nature* **498**, 201 (2013).
- [10] C. V. Parker, L.-C. Ha, and C. Chin, *Nature Physics* **9**, 769 (2013).
- [11] K. Jiménez-García, L. J. LeBlanc, R. A. Williams, M. C. Beeler, C. Qu, M. Gong, C. Zhang, and I. B. Spielman, *Phys. Rev. Lett.* **114**, 125301 (2015), URL <https://link.aps.org/doi/10.1103/PhysRevLett.114.125301>.
- [12] L. W. Clark, L. Feng, and C. Chin, *Science* **354**, 606 (2016).
- [13] A. Putra, F. Salces-Cárcoba, Y. Yue, S. Sugawa, and I. B. Spielman, *Phys. Rev. Lett.* **124**, 053605 (2020), URL <https://link.aps.org/doi/10.1103/PhysRevLett.124.053605>.
- [14] K.-X. Yao, Z. Zhang, and C. Chin, *Nature* **602**, 68 (2022).
- [15] V. Galitski and I. B. Spielman, *Nature* **494**, 49 (2013).
- [16] H. Zhai, *Reports on Progress in Physics* **78**, 026001 (2015).
- [17] N. Goldman, G. Juzeliūnas, P. Öhberg, and I. B. Spielman, *Reports on Progress in Physics* **77**, 126401 (2014).
- [18] M. Atala, M. Aidelsburger, M. Lohse, J. T. Barreiro, B. Paredes, and I. Bloch, *Nature Physics* **10**, 588 (2014).
- [19] A. Celi, P. Massignan, J. Ruseckas, N. Goldman, I. B. Spielman, G. Juzeliūnas, and M. Lewenstein, *Phys. Rev. Lett.* **112**, 043001 (2014), URL <https://link.aps.org/doi/10.1103/PhysRevLett.112.043001>.
- [20] A. Dhar, M. Maji, T. Mishra, R. V. Pai, S. Mukerjee, and A. Paramekanti, *Phys. Rev. A* **85**, 041602 (2012), URL <https://link.aps.org/doi/10.1103/PhysRevA.85.041602>.
- [21] T.-L. Ho and S. Zhang, *Phys. Rev. Lett.* **107**, 150403 (2011), URL <https://link.aps.org/doi/10.1103/PhysRevLett.107.150403>.
- [22] Y. Li, L. P. Pitaevskii, and S. Stringari, *Phys. Rev. Lett.* **108**, 225301 (2012), URL <https://link.aps.org/doi/10.1103/PhysRevLett.108.225301>.
- [23] H. Hu, B. Ramachandhran, H. Pu, and X.-J. Liu, *Phys. Rev. Lett.* **108**, 010402 (2012), URL <https://link.aps.org/doi/10.1103/PhysRevLett.108.010402>.
- [24] W. S. Cole, S. Zhang, A. Paramekanti, and N. Trivedi, *Phys. Rev. Lett.* **109**, 085302 (2012), URL <https://link.aps.org/doi/10.1103/PhysRevLett.109.085302>.
- [25] C. Qu, C. Hamner, M. Gong, C. Zhang, and P. Engels, *Phys. Rev. A* **88**, 021604 (2013), URL <https://link.aps.org/doi/10.1103/PhysRevA.88.021604>.
- [26] W. Zheng, B. Liu, J. Miao, C. Chin, and H. Zhai, *Phys. Rev. Lett.* **113**, 155303 (2014), URL <https://link.aps.org/doi/10.1103/PhysRevLett.113.155303>.
- [27] Z. Xu, W. S. Cole, and S. Zhang, *Phys. Rev. A* **89**, 051604 (2014), URL <https://link.aps.org/doi/10.1103/PhysRevA.89.051604>.
- [28] M. Khamsehchi, C. Qu, M. Mossman, C. Zhang, and P. Engels, *Nature communications* **7**, 10867 (2016).
- [29] T. Liu, L. W. Clark, and C. Chin, *Phys. Rev. A* **94**, 063646 (2016), URL <https://link.aps.org/doi/10.1103/PhysRevA.94.063646>.
- [30] W. S. Cole, J. Lee, K. W. Mahmud, Y. Alavirad, I. Spielman, and J. D. Sau, *Scientific Reports* **9**, 7471 (2019).
- [31] E. Orignac, R. Citro, M. Di Dio, and S. De Palo, *Phys. Rev. B* **96**, 014518 (2017), URL <https://link.aps.org/doi/10.1103/PhysRevB.96.014518>.
- [32] A. Tokuno and A. Georges, *New Journal of Physics* **16**, 073005 (2014).
- [33] H. C. Po, W. Chen, and Q. Zhou, *Phys. Rev. A*

- 90, 011602 (2014), URL <https://link.aps.org/doi/10.1103/PhysRevA.90.011602>.
- [34] H. C. Po and Q. Zhou, Nature Communications **6**, 8012 (2015).
- [35] J. Radić, S. S. Natu, and V. Galitski, Phys. Rev. A **91**, 063634 (2015), URL <https://link.aps.org/doi/10.1103/PhysRevA.91.063634>.
- [36] S. Sur and K. Yang, Phys. Rev. B **100**, 024519 (2019), URL <https://link.aps.org/doi/10.1103/PhysRevB.100.024519>.
- [37] E. Lake, T. Senthil, and A. Vishwanath, Phys. Rev. B **104**, 014517 (2021), URL <https://link.aps.org/doi/10.1103/PhysRevB.104.014517>.
- [38] C. Chamon, Phys. Rev. Lett. **94**, 040402 (2005), URL <https://link.aps.org/doi/10.1103/PhysRevLett.94.040402>.
- [39] C. Castelnovo and C. Chamon, Philosophical Magazine **92**, 304 (2012).
- [40] J. Haah, Phys. Rev. A **83**, 042330 (2011), URL <https://link.aps.org/doi/10.1103/PhysRevA.83.042330>.
- [41] S. Vijay, J. Haah, and L. Fu, Phys. Rev. B **94**, 235157 (2016), URL <https://link.aps.org/doi/10.1103/PhysRevB.94.235157>.
- [42] M. Pretko, Phys. Rev. B **95**, 115139 (2017), URL <https://link.aps.org/doi/10.1103/PhysRevB.95.115139>.
- [43] M. Pretko, Phys. Rev. B **96**, 035119 (2017), URL <https://link.aps.org/doi/10.1103/PhysRevB.96.035119>.
- [44] A. Prem, J. Haah, and R. Nandkishore, Phys. Rev. B **95**, 155133 (2017), URL <https://link.aps.org/doi/10.1103/PhysRevB.95.155133>.
- [45] M. Pretko, Phys. Rev. B **98**, 115134 (2018), URL <https://link.aps.org/doi/10.1103/PhysRevB.98.115134>.
- [46] R. M. Nandkishore and M. Hermele, Annual Review of Condensed Matter Physics **10**, 295 (2019), URL <https://doi.org/10.1146/annurev-conmatphys-031218-013604>.
- [47] M. Pretko, X. Chen, and Y. You, International Journal of Modern Physics A **35**, 2030003 (2020).
- [48] L. Radzihovsky, Phys. Rev. Lett. **125**, 267601 (2020), URL <https://link.aps.org/doi/10.1103/PhysRevLett.125.267601>.
- [49] A. Gromov and L. Radzihovsky, arXiv preprint arXiv:2211.05130 (2022).
- [50] N. Seiberg, SciPost Physics **8**, 050 (2020).
- [51] S. Pai and M. Pretko, Phys. Rev. Res. **2**, 013094 (2020), URL <https://link.aps.org/doi/10.1103/PhysRevResearch.2.013094>.
- [52] E. Lake, M. Hermele, and T. Senthil, Phys. Rev. B **106**, 064511 (2022), URL <https://link.aps.org/doi/10.1103/PhysRevB.106.064511>.
- [53] P. Gorantla, H. T. Lam, N. Seiberg, and S.-H. Shao, Phys. Rev. B **106**, 045112 (2022), URL <https://link.aps.org/doi/10.1103/PhysRevB.106.045112>.
- [54] P. Gorantla, H. T. Lam, N. Seiberg, and S.-H. Shao, arXiv preprint arXiv:2209.10030 (2022).
- [55] P. Zechmann, E. Altman, M. Knap, and J. Feldmeier, Phys. Rev. B **107**, 195131 (2023), URL <https://link.aps.org/doi/10.1103/PhysRevB.107.195131>.
- [56] L. Radzihovsky, Phys. Rev. B **106**, 224510 (2022), URL <https://link.aps.org/doi/10.1103/PhysRevB.106.224510>.
- [57] E. Lake and T. Senthil, arXiv preprint arXiv:2302.08499 (2023).
- [58] E. H. Lieb and W. Liniger, Phys. Rev. **130**, 1605 (1963), URL <https://link.aps.org/doi/10.1103/PhysRev.130.1605>.
- [59] E. H. Lieb, Phys. Rev. **130**, 1616 (1963), URL <https://link.aps.org/doi/10.1103/PhysRev.130.1616>.
- [60] F. D. M. Haldane, Phys. Rev. Lett. **47**, 1840 (1981), URL <https://link.aps.org/doi/10.1103/PhysRevLett.47.1840>.
- [61] P. M. Preiss, R. Ma, M. E. Tai, A. Lukin, M. Rispoli, P. Zupancic, Y. Lahini, R. Islam, and M. Greiner, Science **347**, 1229 (2015).
- [62] T. Giamarchi, *Quantum physics in one dimension* (Oxford Science Publications, Oxford, 2004).
- [63] K. Yang, Phys. Rev. Lett. **93**, 066401 (2004), URL <https://link.aps.org/doi/10.1103/PhysRevLett.93.066401>.
- [64] S. Sachdev and T. Senthil, Annals of Physics **251**, 76 (1996).
- [65] O. A. Castro-Alvaredo, B. Doyon, and T. Yoshimura, Phys. Rev. X **6**, 041065 (2016), URL <https://link.aps.org/doi/10.1103/PhysRevX.6.041065>.
- [66] K. A. Matveev, Phys. Rev. B **102**, 155401 (2020), URL <https://link.aps.org/doi/10.1103/PhysRevB.102.155401>.
- [67] S. Sachdev and A. P. Young, Phys. Rev. Lett. **78**, 2220 (1997), URL <https://link.aps.org/doi/10.1103/PhysRevLett.78.2220>.
- [68] S. Sachdev, Physics world **12**, 33 (1999).
- [69] Z.-C. Yang, F. Liu, A. V. Gorshkov, and T. Iadecola, Phys. Rev. Lett. **124**, 207602 (2020), URL <https://link.aps.org/doi/10.1103/PhysRevLett.124.207602>.
- [70] A. Bastianello, U. Borla, and S. Moroz, Phys. Rev. Lett. **128**, 196601 (2022), URL <https://link.aps.org/doi/10.1103/PhysRevLett.128.196601>.
- [71] V. Khemani, M. Hermele, and R. Nandkishore, Phys. Rev. B **101**, 174204 (2020), URL <https://link.aps.org/doi/10.1103/PhysRevB.101.174204>.
- [72] P. Sala, T. Rakovszky, R. Verresen, M. Knap, and F. Pollmann, Phys. Rev. X **10**, 011047 (2020), URL <https://link.aps.org/doi/10.1103/PhysRevX.10.011047>.
- [73] T. Rakovszky, P. Sala, R. Verresen, M. Knap, and F. Pollmann, Phys. Rev. B **101**, 125126 (2020), URL <https://link.aps.org/doi/10.1103/PhysRevB.101.125126>.
- [74] G. De Tomasi, D. Hetterich, P. Sala, and F. Pollmann, Phys. Rev. B **100**, 214313 (2019), URL <https://link.aps.org/doi/10.1103/PhysRevB.100.214313>.
- [75] S. Moudgalya and O. I. Motrunich, Phys. Rev. X **12**, 011050 (2022), URL <https://link.aps.org/doi/10.1103/PhysRevX.12.011050>.
- [76] T. Kohler, S. Scherg, P. Sala, F. Pollmann, B. H. Madhusudhana, I. Bloch, and M. Aidelsburger, arXiv preprint arXiv:2106.15586 (2021).
- [77] B. Mukherjee, D. Banerjee, K. Sengupta, and A. Sen, Phys. Rev. B **104**, 155117 (2021), URL <https://link.aps.org/doi/10.1103/PhysRevB.104.155117>.
- [78] S. Ghosh, I. Paul, and K. Sengupta, Physical Review Letters **130**, 120401 (2023).
- [79] Z. Lan, M. van Horssen, S. Powell, and J. P. Garrahan, Phys. Rev. Lett. **121**, 040603 (2018), URL <https://link.aps.org/doi/10.1103/PhysRevLett.121.040603>.
- [80] V. Kozii, J. Ruhman, L. Fu, and L. Radzihovsky, Phys. Rev. B **96**, 094419 (2017), URL <https://link.aps.org/doi/10.1103/PhysRevB.96.094419>.
- [81] A. Kamenev and A. Levchenko, Advances in Physics **58**, 197 (2009).

- [82] A. Kamenev, *Field theory of non-equilibrium systems* (Cambridge University Press, 2023).
- [83] C. Hoyos, B. S. Kim, and Y. Oz, *Journal of High Energy Physics* **2013**, 1 (2013).
- [84] C. Hoyos, B. S. Kim, and Y. Oz, *Journal of High Energy Physics* **2014**, 1 (2014).